# Focusing on the flame

## Some practical tips for flame diagnostics

Yuriy Shoshin

Eindhoven University of Technology

Members Meeting of the Dutch Section of Combustion Institute. TU/e, 26/01/2024

# Presentation content

- Particle Image Velocimetry (PIV)
- Interferometry for flames
    - Regular interferometry
    - Holographic interferometry
    - Digital holographic interferometry
- Laser attenuation measurements for solid/liquid aerosols
- In-line particle size measurement by light attenuation
- Rayleigh scattering for flames in small confinements
- Problems of color/multispectral camera pyrometry for dust flames

# Particle Image Velocimetry. How it works?

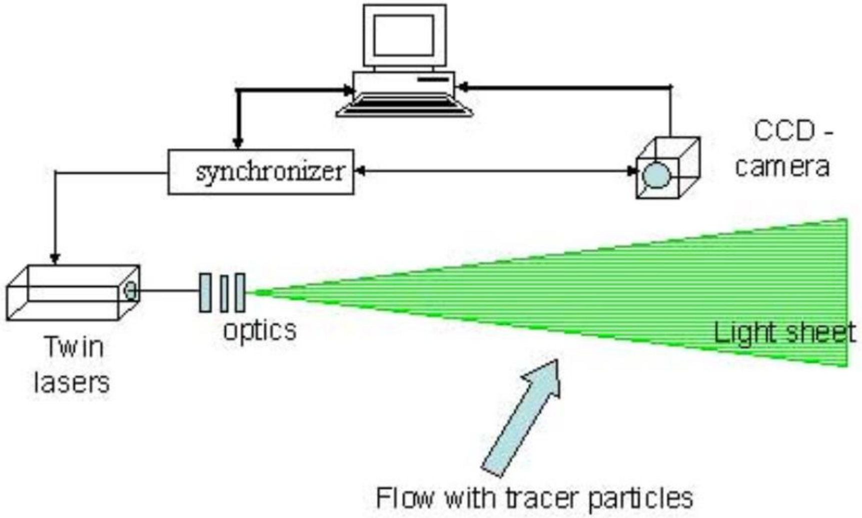


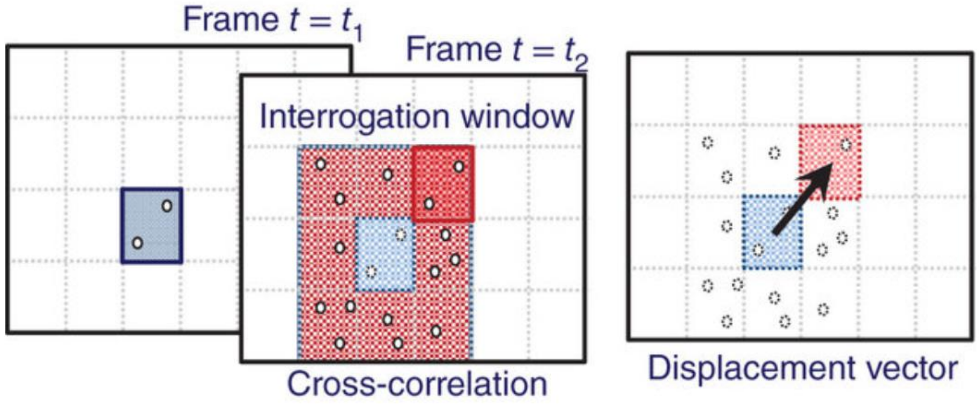


- Seeded flow is illuminated with a (pulsed) laser sheet.
- **Cross correlation.** Two consecutive images are taken with a known delay time.
- Software splits the first image onto small interrogation windows. It is shifted in all directions and is compared to the corresponding shifted window on the second image. The best match (correlation) corresponds to the local particle displacement between the two laser pulses.
  - The image can be crowded with particles so you may not be able to tell one particle from another. Do not worry, it will work only better, providing higher resolution and fewer outliers.
- **Auto-correlation.** Two (or more) PIV images are exposed on the same frame. Interrogation windows are shifted over the same image. When looking for correlation, zero displacement is excluded.
  - Auto-correlation can be advantageous in many cases.

# Particle Image Velocimetry. What can be measured?

- Local burning velocity.
- Local and net flame stretch rate, $\frac{1}{A} \cdot \frac{dA}{dt}$ ($A$ is the area of a small element of the flame front).
- Local or global dilatation rate, $\frac{1}{V}\frac{dV}{dt} = \nabla \cdot \vec{v}$ ($V$ is a small volume).
  - Locations of the beginning of the flame preheat zone and end of the reaction zone.
  - Local heat release rate per unit of the flame front area.
- Total heat release rate (minus radiation losses), when the whole flame is in the field of view.
- Temperature field for steady state or steadily propagating flames.
  - Streamlines must be determined precisely for this (no outliers).

+ more…

# PIV. Pros and cons of auto-correlation method.

- Modulated laser illuminates particles and consecutive images of the same particle are taken on a single frame
  - A cheap laser diode can be used. Modulation frequency up to 100-250 kHz.
  - A camera with a global shutter is preferable to use. For small velocities, a rolling shutter is also OK.
  - A regular camera can have a much higher resolution than a PIV camera.
- **For steady-state flames**, multiple, e.g. $n$ = 50, images of the same particle can be taken which is equivalent to the increase of seeding number density $n/2$ times.
  - Particle number density can be reduced to avoid their effect on the flame and the resolution and precision of velocity field measurement can be improved simultaneously.
- For steady-state flames, better quality measurements can be performed without using expensive special equipment (PIV lasers or PIV cameras).

- Velocity direction can not be determined, but it is usually known.

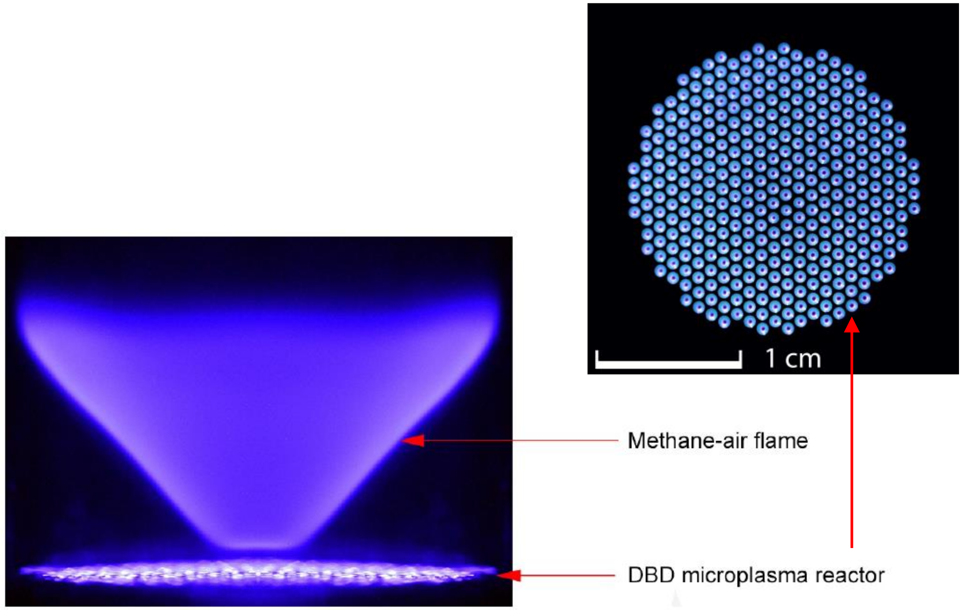


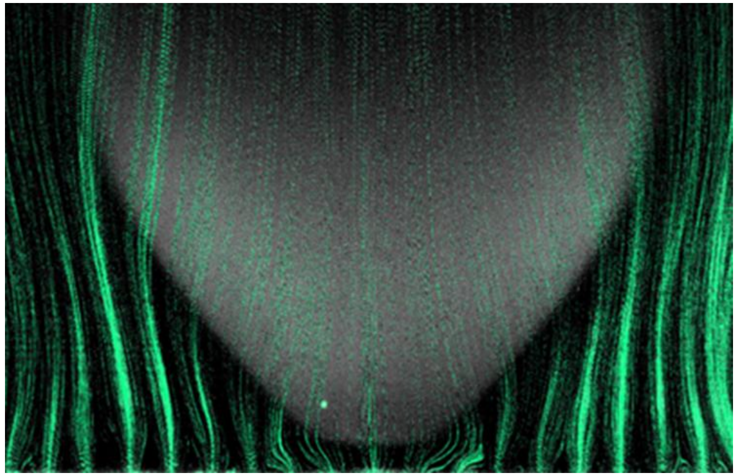

(Elkholy, A. H. E., PhD Thesis, 2019)PhD

# Particle Image Velocimetry. Parallel focused laser sheet.

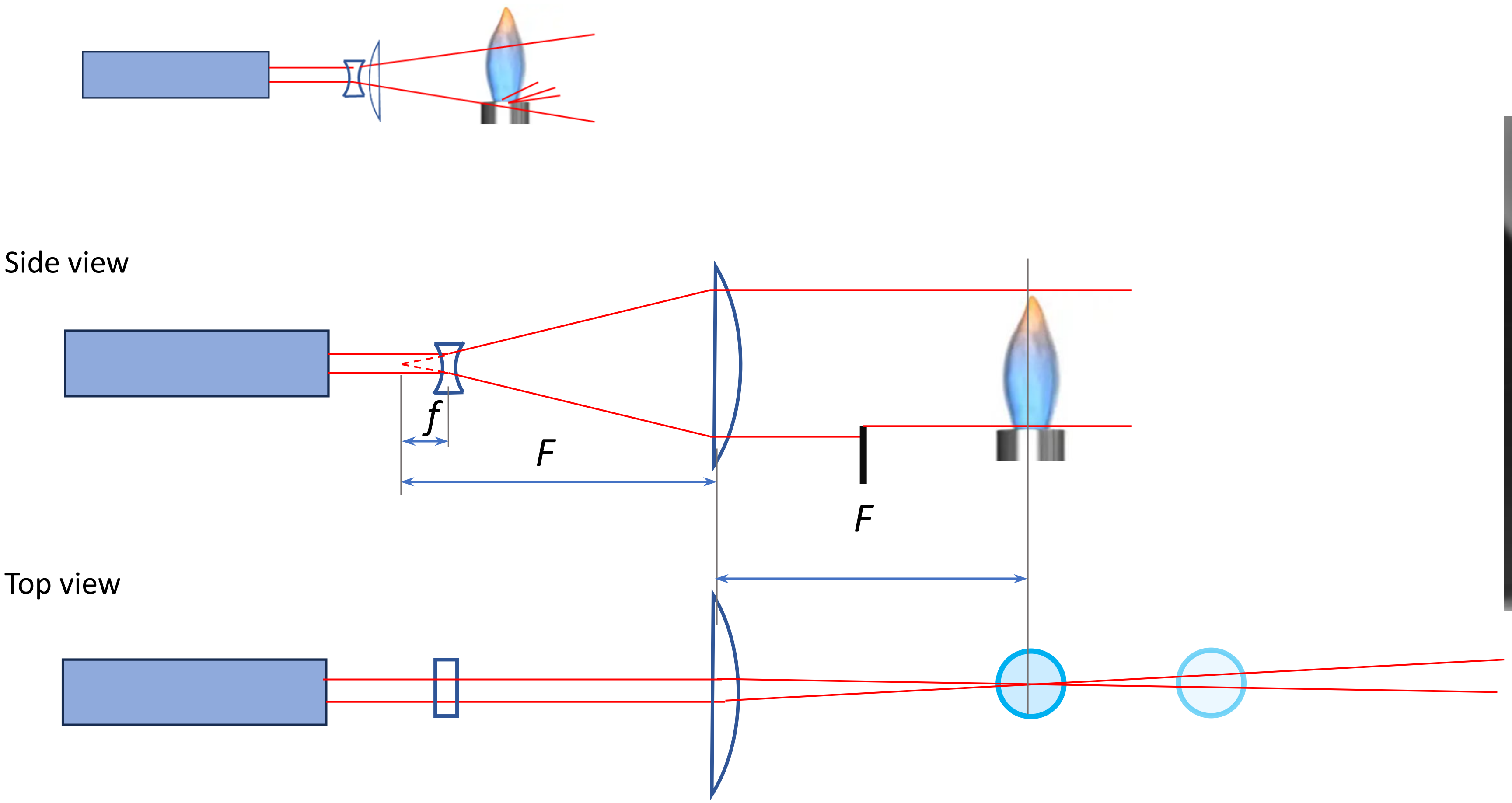


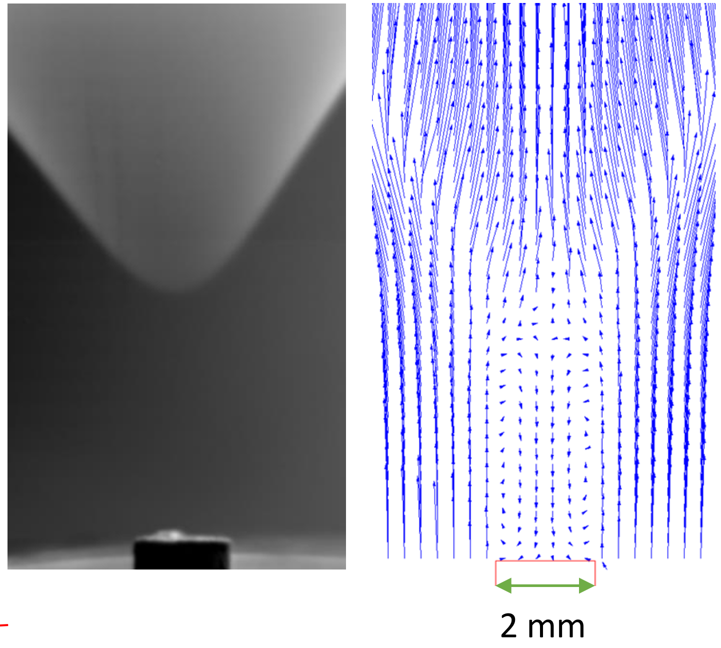


- Thin laser sheet (can be made thicker by moving the flame out of focus).
- Measurements very close to a burner rim/surface are possible.
    - Use an achromatic-, or camera lens. A plano-convex lens can be used, though the laser sheet may be thicker.

## PIV in transparent tubes.

1. Simple solution

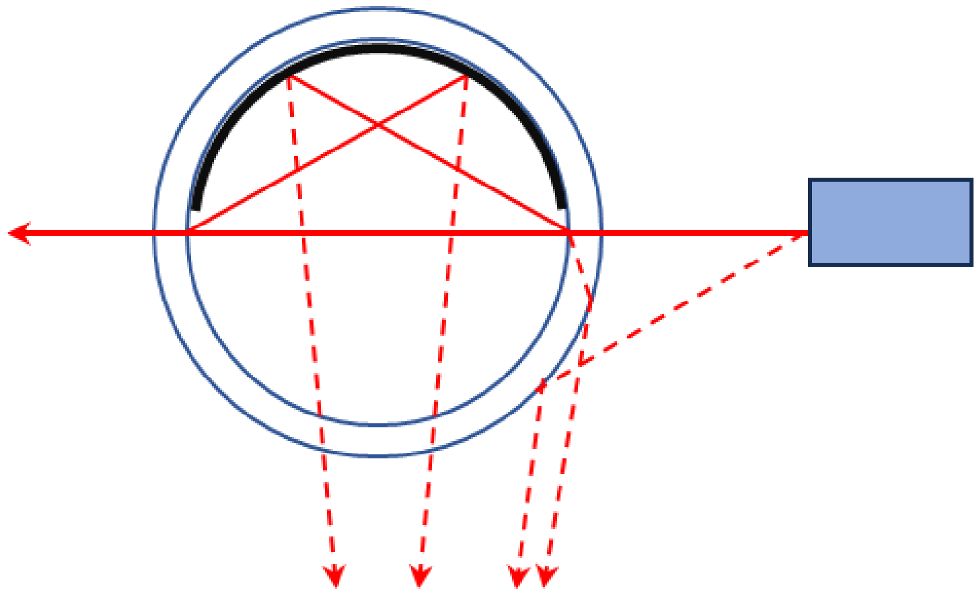

To PIV camera

2. Ultimate solution

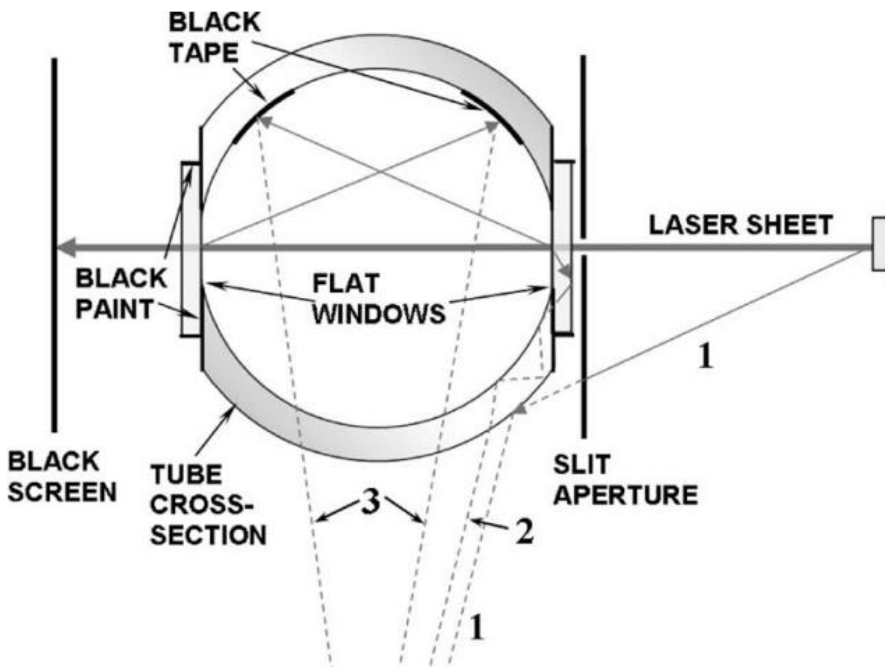


To PIV camera

- A simple solution will work in most cases. It does not remove bright strips near the wall, but usually, there is a dead zone there.
- If the tube gets very hot, black paint for car mufflers can be used (up to 900°C).

# Stream tube method for measuring local burning velocity for steady for steadily propagating flames

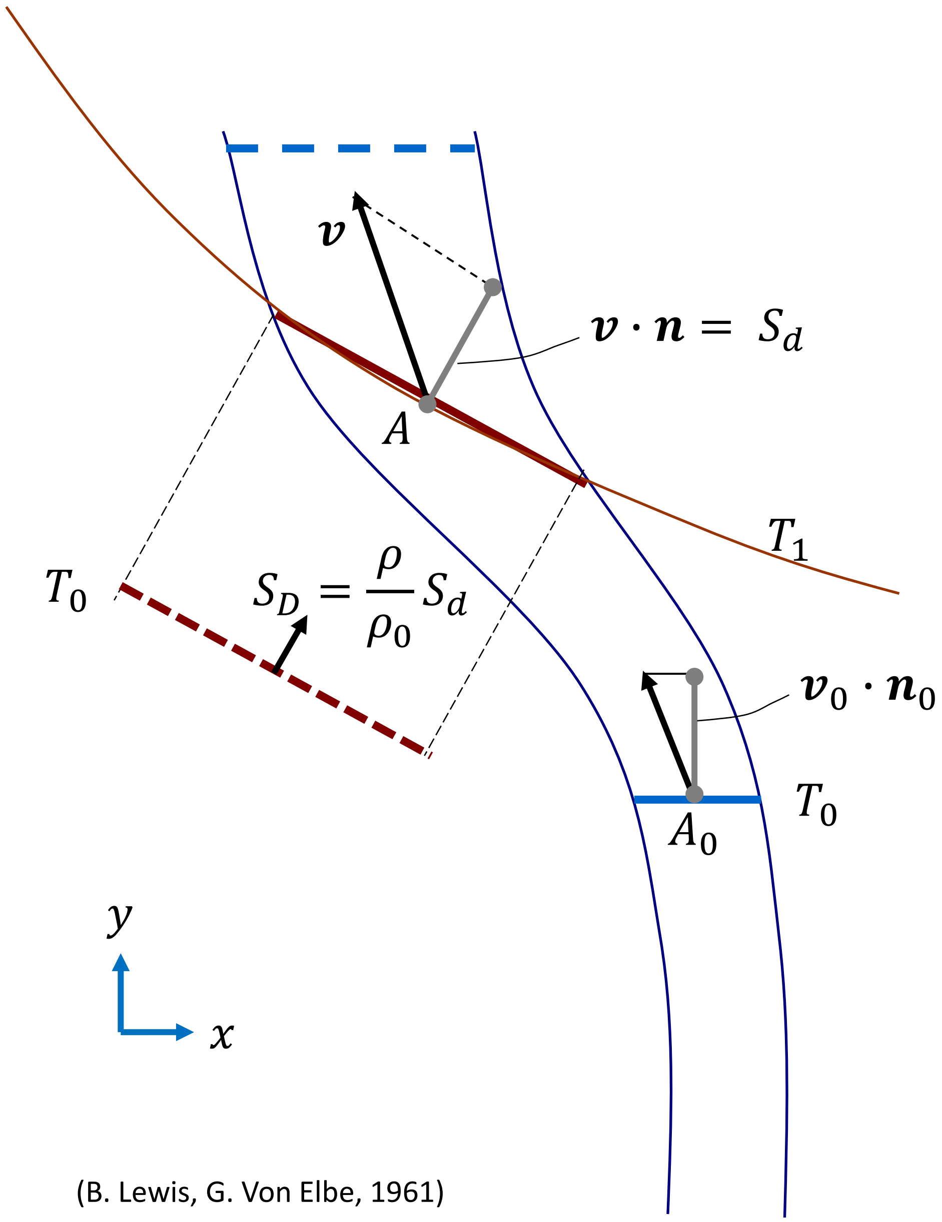


(B. Lewis, G. Von Elbe, 1961)

Measured velocity field: $u_x(x, y); u_y(x, y)$

$$S_d = (\boldsymbol{V}_f - \boldsymbol{v}) \cdot \boldsymbol{n} \quad (1)$$

$$S_D = \frac{\rho}{\rho_0} S_d \quad (2)$$

Most relevant location for measuring local burning velocity is the reaction zone. But gas density is affected by the thermal expansion there, and, in general, is unknown.

For a steady-state flame:

$$\boldsymbol{V}_f = 0; \quad S_d = (-)\boldsymbol{v} \cdot \boldsymbol{n} \quad (3)$$

Continuity:

$$\rho_0 \cdot (\boldsymbol{v}_0 \cdot \boldsymbol{n}_0) \cdot A_0 = \rho \cdot (\boldsymbol{v} \cdot \boldsymbol{n}) \cdot A \quad (4)$$

From Eq. 2, 3, 4:

$$\boxed{S_D = \boldsymbol{v}_0 \cdot \boldsymbol{n}_0 \frac{A_0}{A} = u_{y,0} \cdot \frac{A_0}{A}}$$

# Stream tube method, example #1: limit methane-air flame in a standard flammability tube (50 mm dia.)


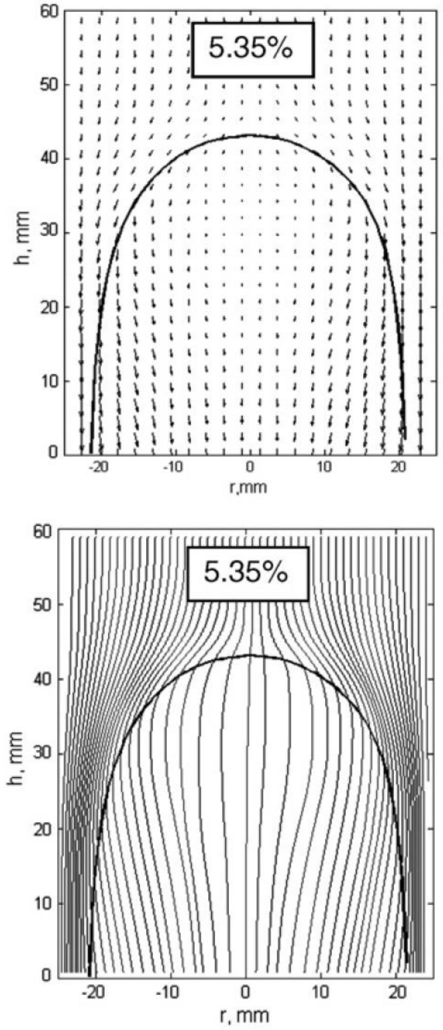


Velocity field (top) and streamlines (bottom ) after the flame propagation speed substruction

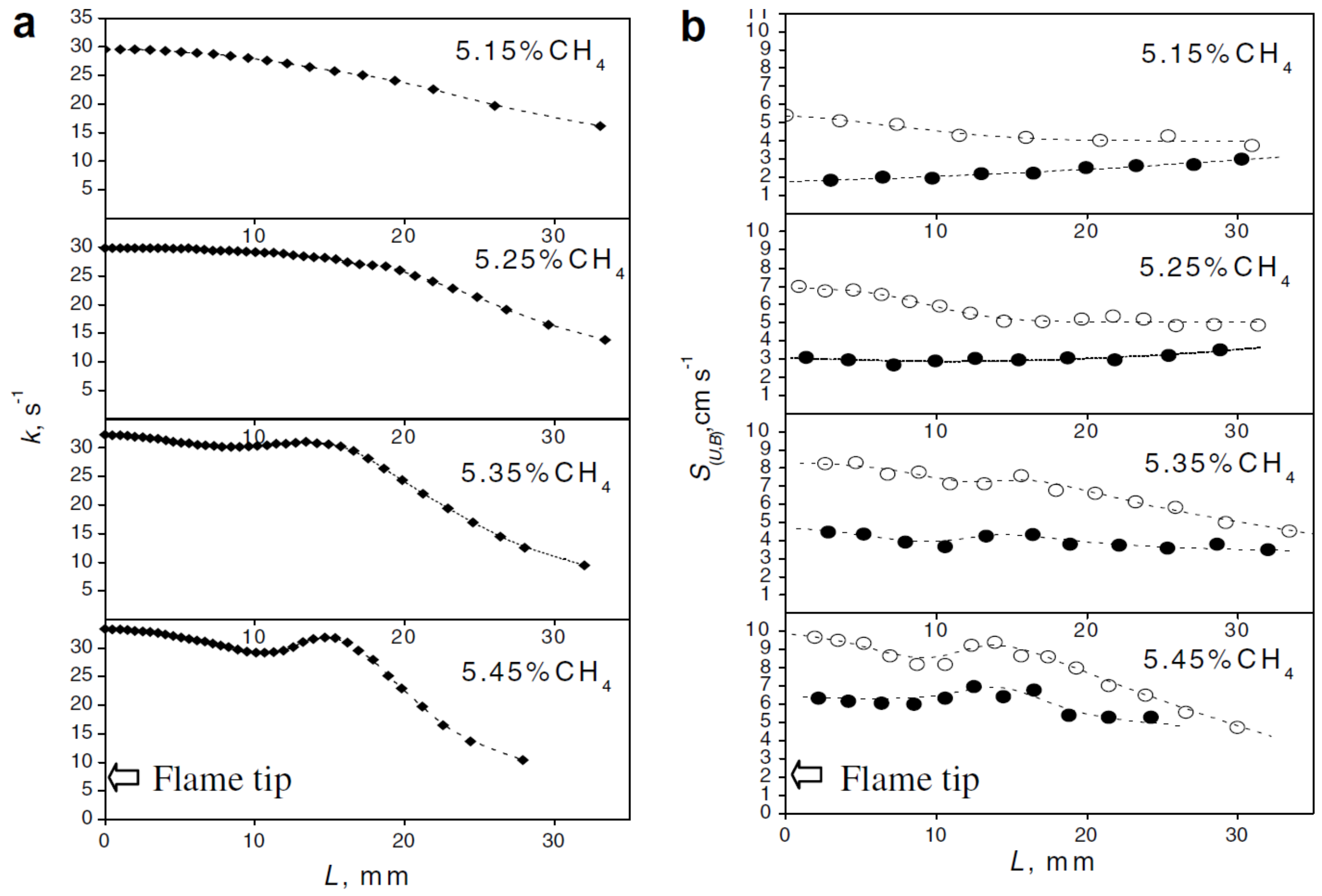


Local stretch rates (left) and burning velocities (right) relative to cold () and hot boundaries. Cold and hot boundaries are determined by local dilatation rates.

(Y. Shoshin, J. Jarosinski, 2009

# Stream tube method, example #2: studying effect of DBD plasma on burning velocity.

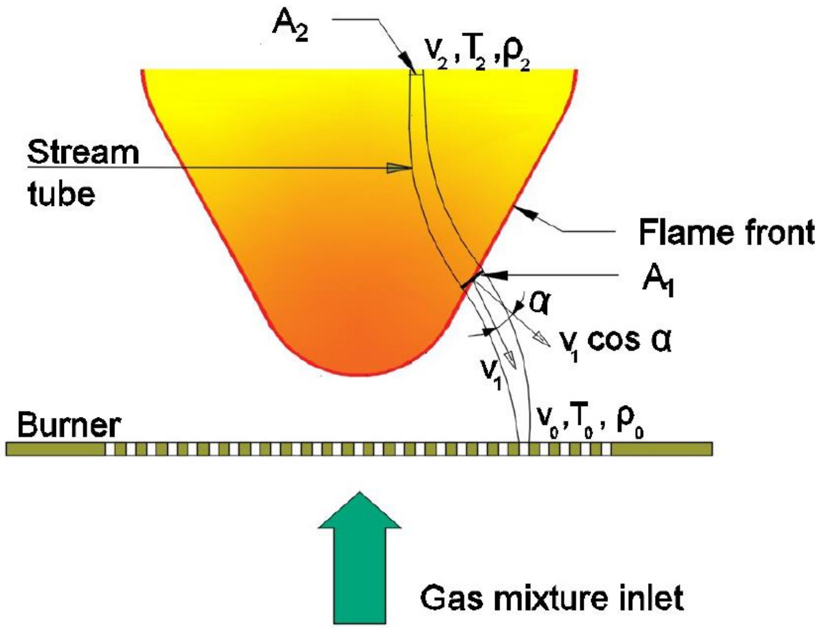


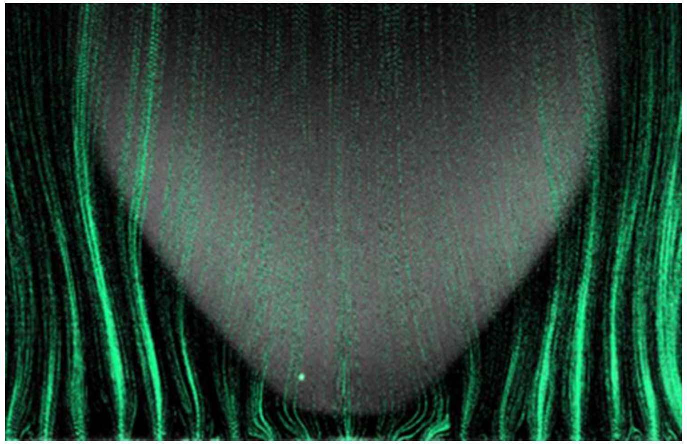

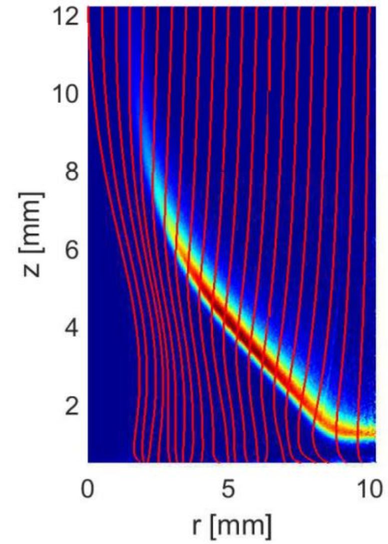


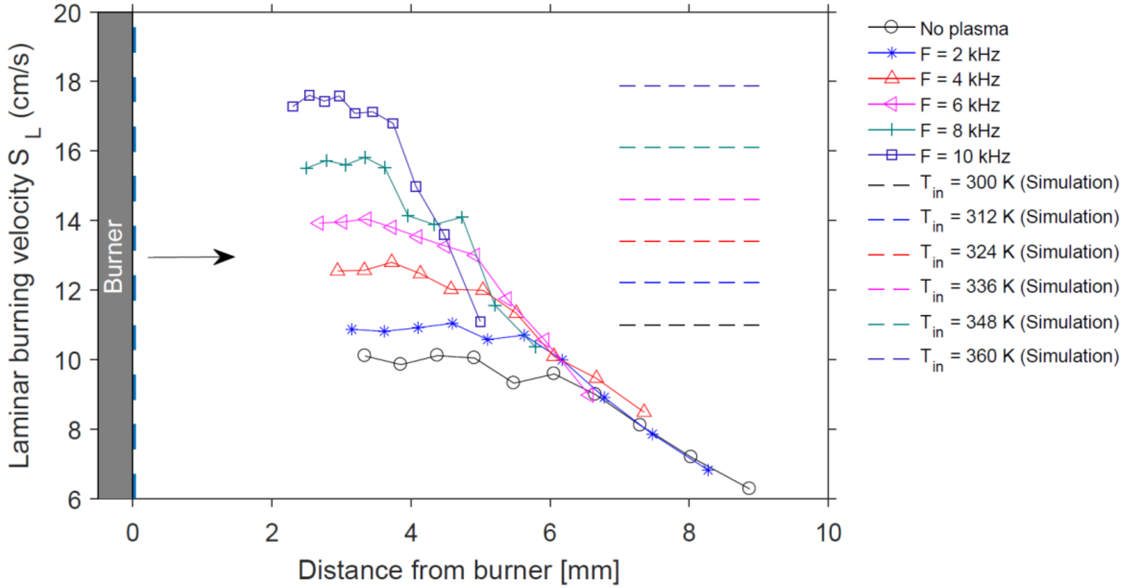


- Auto-correlation mode is used with a high-resolution camera.
- Each particle is exposed ~50 times on one frame.
  - Low seeding density; no effect on plasma.
- Reference temperatures are measured above the flame, in combustion products.

$$S_D = \boldsymbol{v_2} \cdot \boldsymbol{n}_2 \frac{A_2}{A} \cdot \frac{T_0}{T_2} = u_{y,2} \cdot \frac{A_2}{A} \cdot \frac{T_0}{T_2}$$

(Elkholy, A. H. E. (2019). Phd Thesis)

# Temperature field for steady or steadily propagating flames by PIV.

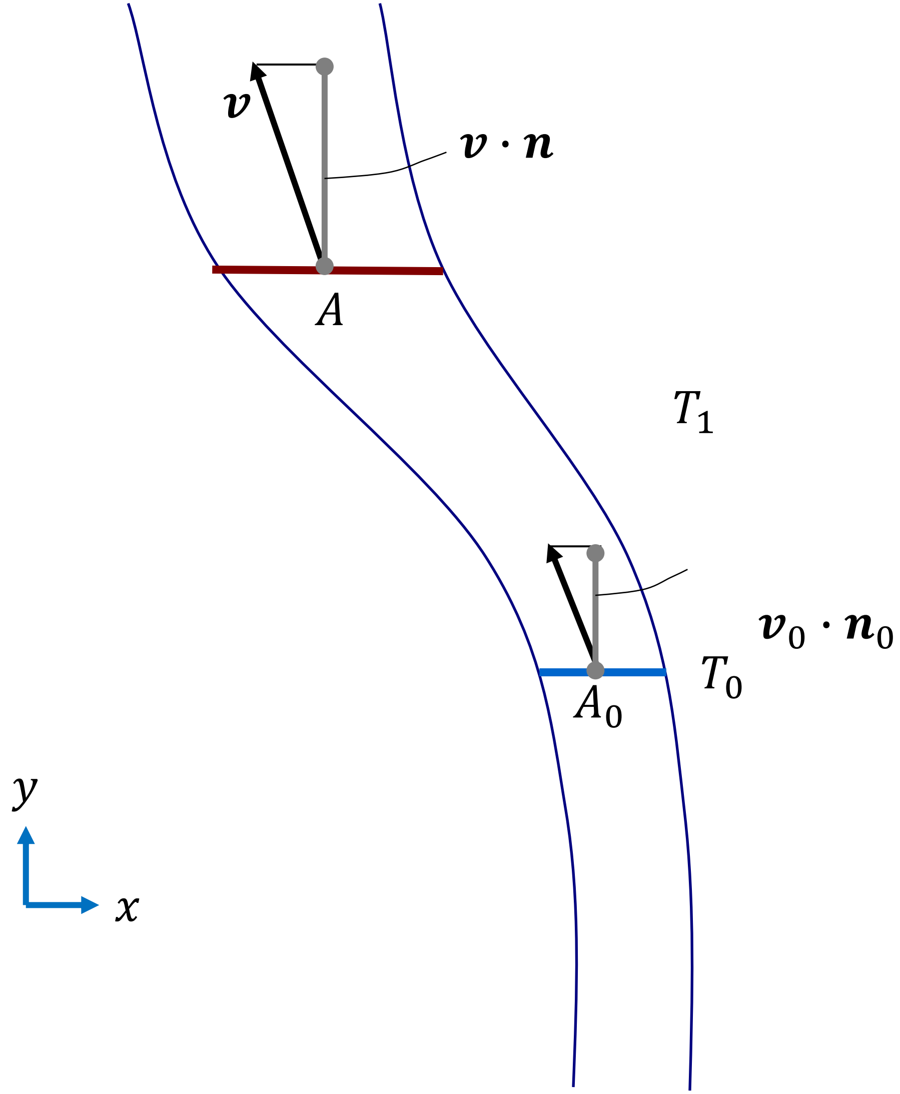


Measured velocity field: $u_x(x,y); u_y(x,y)$

Continuity:

$$\rho_0 \cdot (\boldsymbol{v}_0 \cdot \boldsymbol{n}_0) \cdot A_0 = \rho \cdot (\boldsymbol{v} \cdot \boldsymbol{n}) \cdot A$$

$$\rho_0 u_{y,o} A_0 = \rho u_y A$$

$$\boxed{T \approx T_0 \cdot \frac{\rho_0}{\rho} = \frac{u_y A}{u_{y,o} A_0}}$$

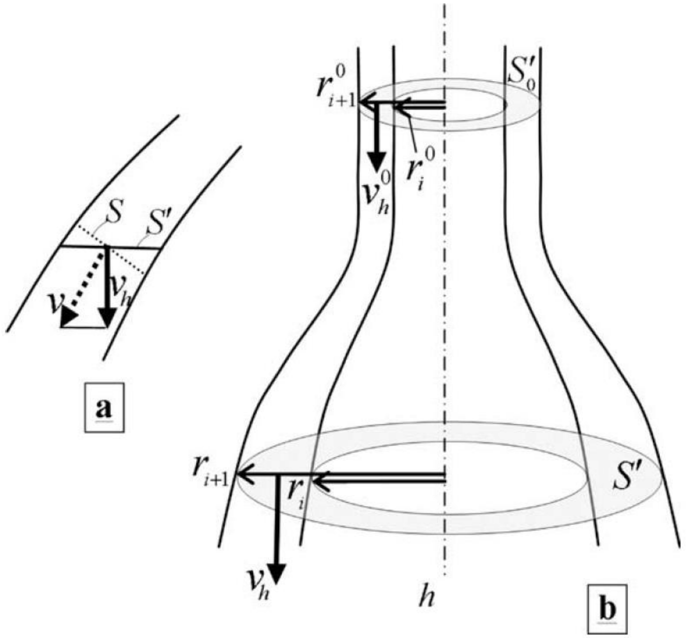


(L. Rimai, K.A. Marko, D. Klick, Proc. Combust. Inst. 19 (1982) 259–265)

# PIV for measurements in counterflow flames. Existing approach.

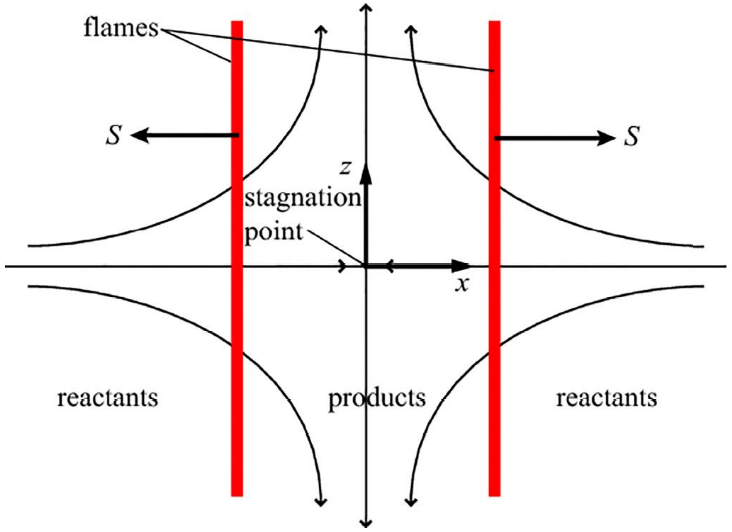


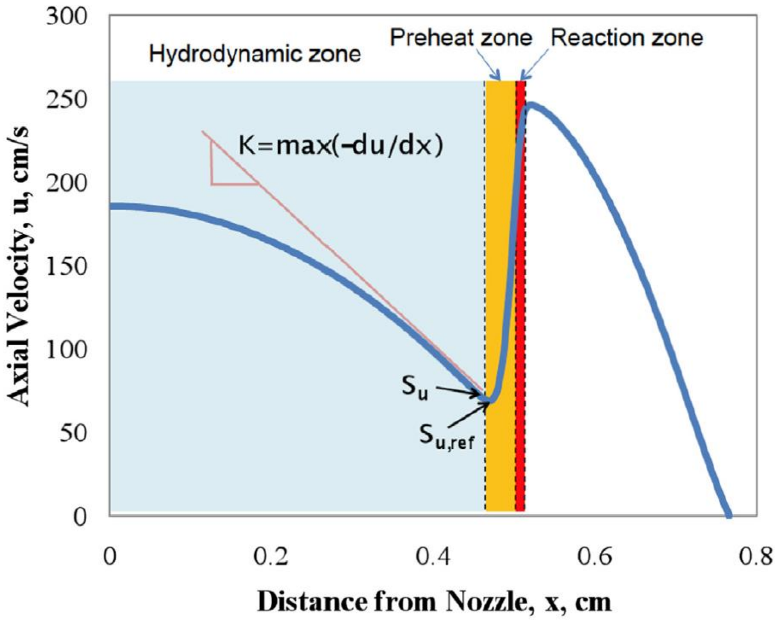


**Axial velocity along the flame centerline**.

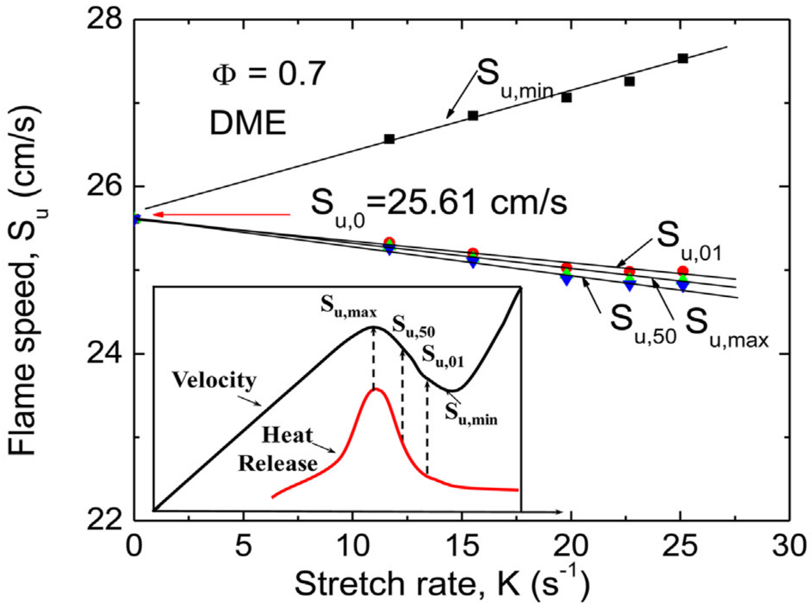


**Measured "reference" burning velocities $S_{u,min}$ (▪) and numerically predicted ones for different iso-levels of heat release rate versus stretch rare.**

- Measured by PIV minimum gas velocity from the cold side, $S_{u,ref}$ is taken as a characteristic "reference" burning velocity.
  - $S_{u,ref}$ is affected by the thermal expansion.
  - The location of the minimum velocity is affected by the flame stretch.
- Maximum value of the axial velocity gradient at the cold side is taken as a characteristic stretch rate
- Preferential diffusion effects are determined by stretch rates within the diffusion thickness of the flame, which can vary .

- Burning velocity is not sensitive to a particular choice of iso-level of the reaction rate downstream of the max. reaction rate location.

(F.N. Egolfopoulos et al., 2014)

# PIV for measurements in counterflow flames. Stream tubes method (newer used).

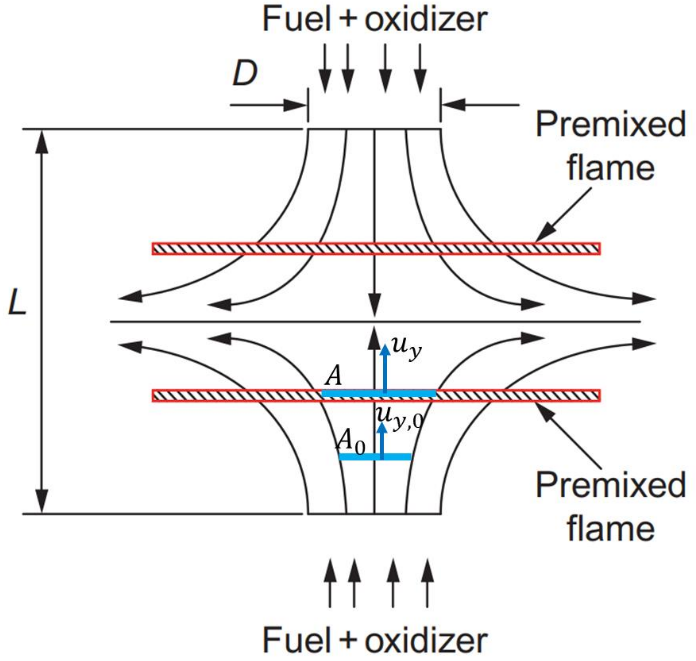


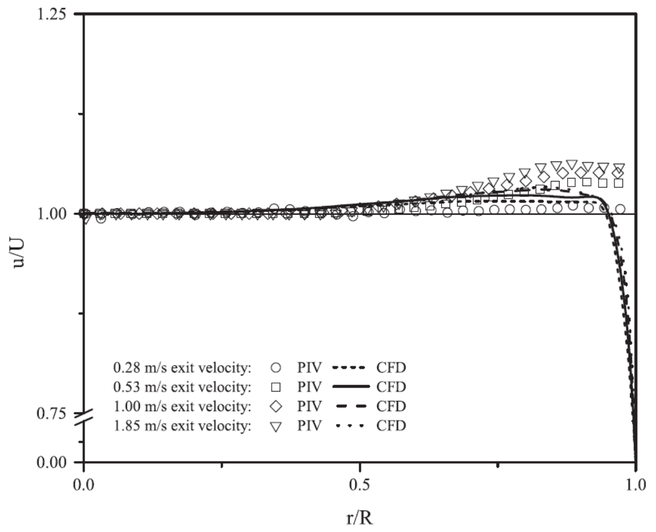


The radial profiles of axial velocity at fixed L

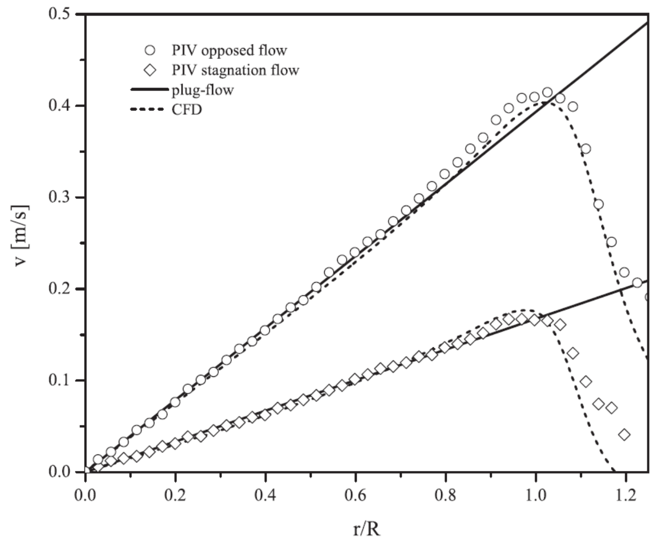


The radial profile of radial velocity at fixed L

(U. Niemann et al., 2015)

Local burning velocity: $S_D = u_{y,0} \cdot \frac{A_0}{A}$

Temperature field: $T \approx T_0 \cdot \frac{\rho_0}{\rho} = \frac{u_y A}{u_{y,o} A_0}$

- Over about half of the whole flame diameter, the flame front and isotherms are flat and $u_y$ is constant at each horizontal level.
- A single wide stream tube can be selected.
  - Simple processing.
  - Smaller error.

- Thermophoresis and particle lag may affect measurements.
- Temperature field (first iteration) can be determined, and error corrected.

# Interferometry for flames. Mach-Zehnder interferometer.

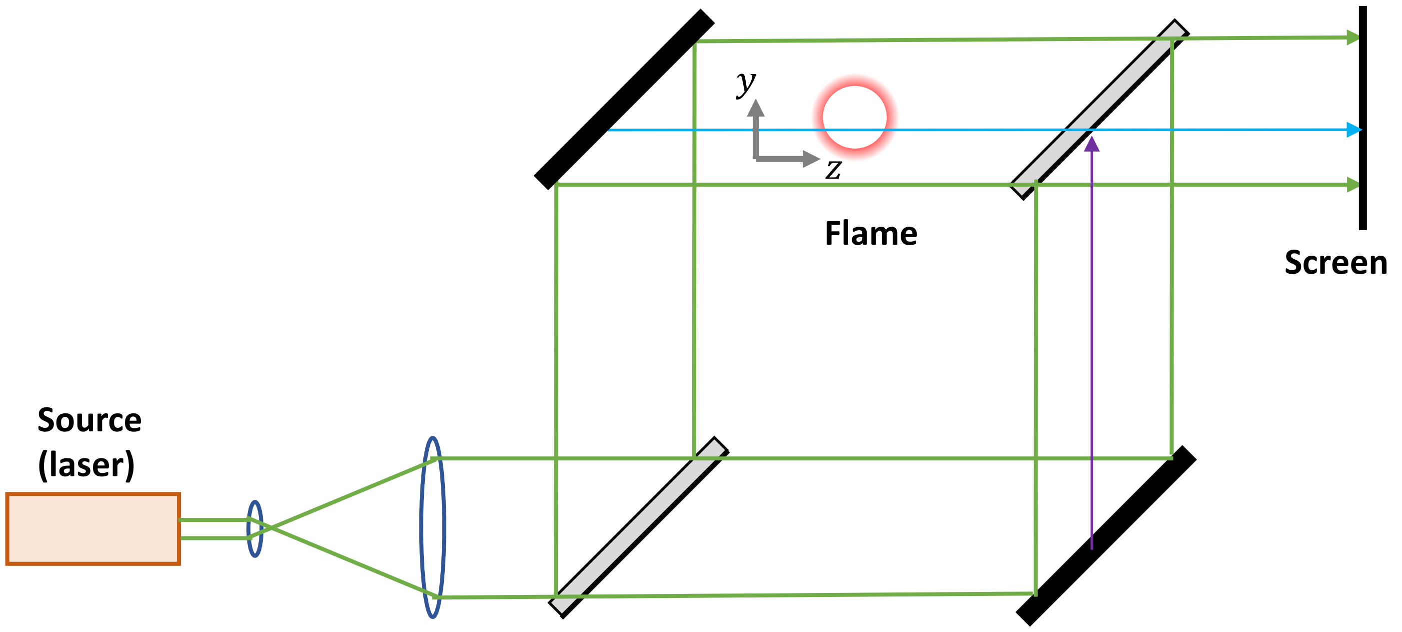


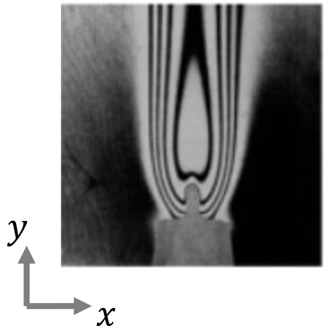


- A parallel light beam is split into two separate beams and then the two beams are combined producing a "flat" interference pattern on a screen.
- When the flame is present in one beam, it changes the refraction index, and local phase differences appear between the two beams:

$$\Delta\varphi = \frac{2\pi}{\lambda}\int [n(x,y,z) - n_0]dz$$

- For $\Delta\varphi = 0, 2\pi, 4\pi$ … white fringes are formed, and for $\Delta\varphi = 1, 3\pi, 5\pi$ … - black fringes
- By counting fringes, the local phase shift is determined.
- For cylindrically symmetric flames, $n(r) - 1$ can be found at every $y$ level using Abel inversion.
- From $n - 1 = k_{mix}\rho_{mix}$ and ideal gas law, temperature can be determined ($k_{mix}$ is Gladstone-Dale constant)
- Nano-particles also affect the refraction index.

# Interferometry for flames. The problem of light deflection by flame.

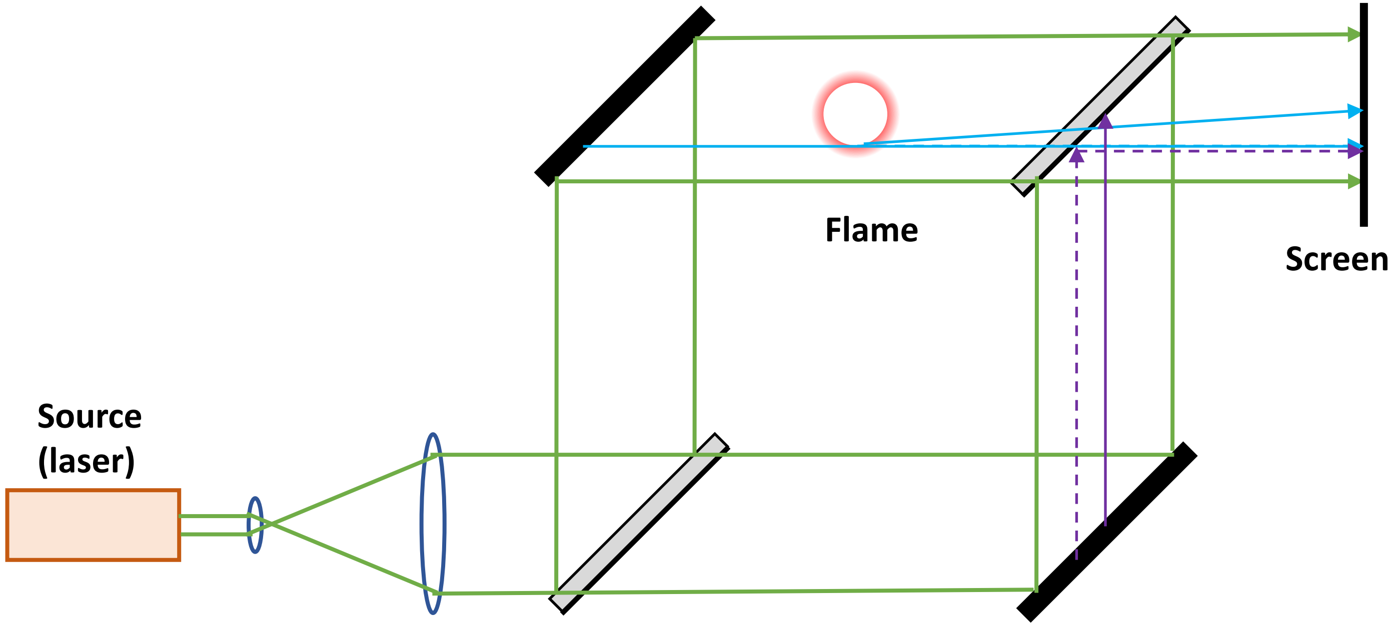


Mach-Zehnder-interferometer

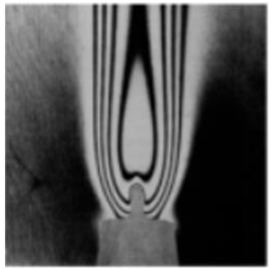

- There are strong density gradients in premixed flames.
- Rays of the measurement wave that travel through the preheat zone can be deflected.
- Interference occurs at non-corresponding locations, which can lead to large errors.

# Interferometry for flames. Focused image interferogram.

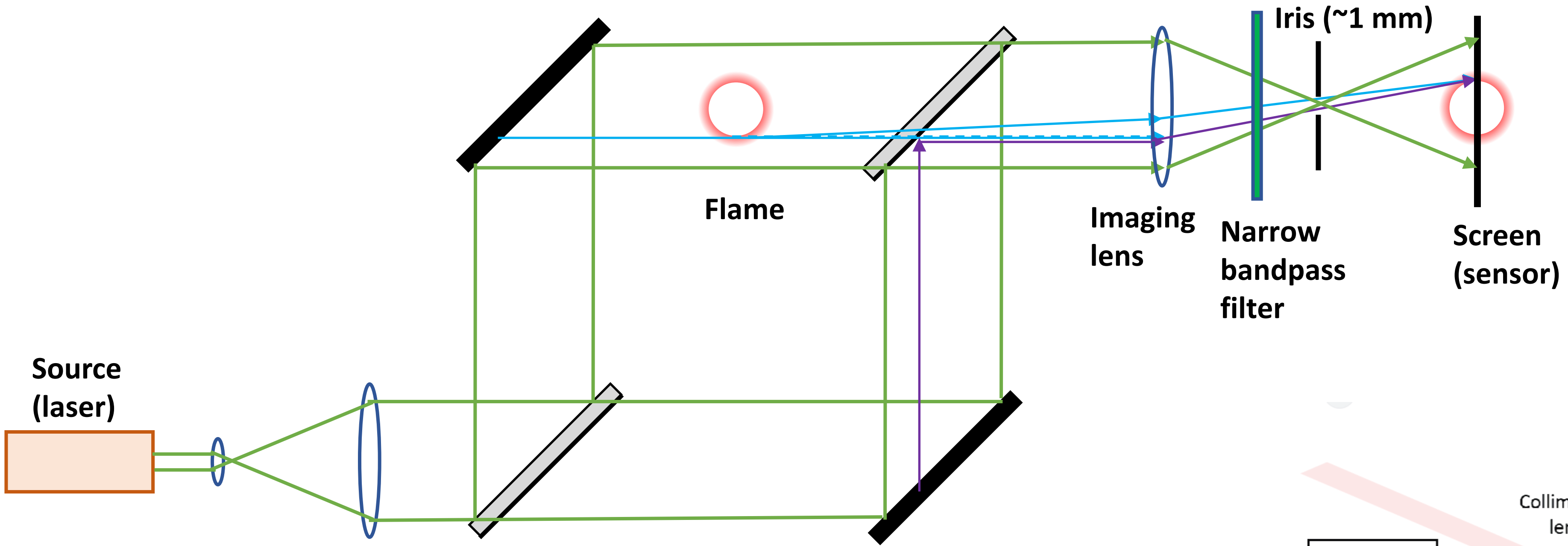


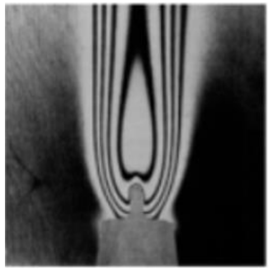

- An imaging lens is added, focused on the flame location.
- All distortions introduced by rays deflection in the measuring beam are removed.
- The measuring and comparison beams interfere at corresponding locations.
- An iris aperture can be placed at the focal distance of the lens. Almost all flame radiation and scattered laser radiation will be removed.
- A narrow band pass filter can be added for very bright flames (metals.)

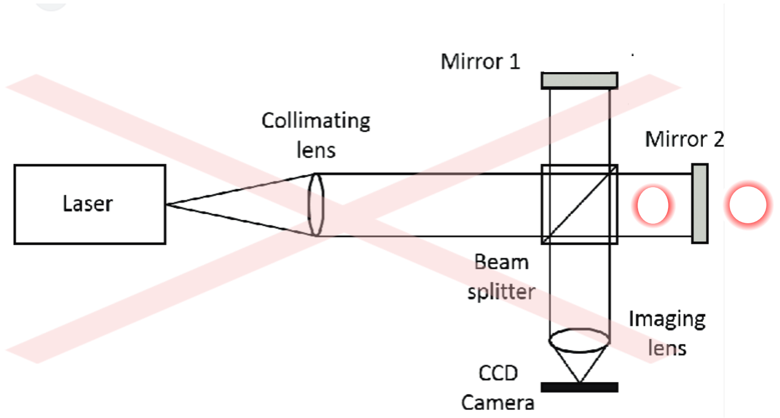


**Twyman–Green interferometer**

- The test beam travels through the flame twice.
- A focused image can not be produced.
- Should not be used for premixed flames.

# Interferometry with finite fringes.

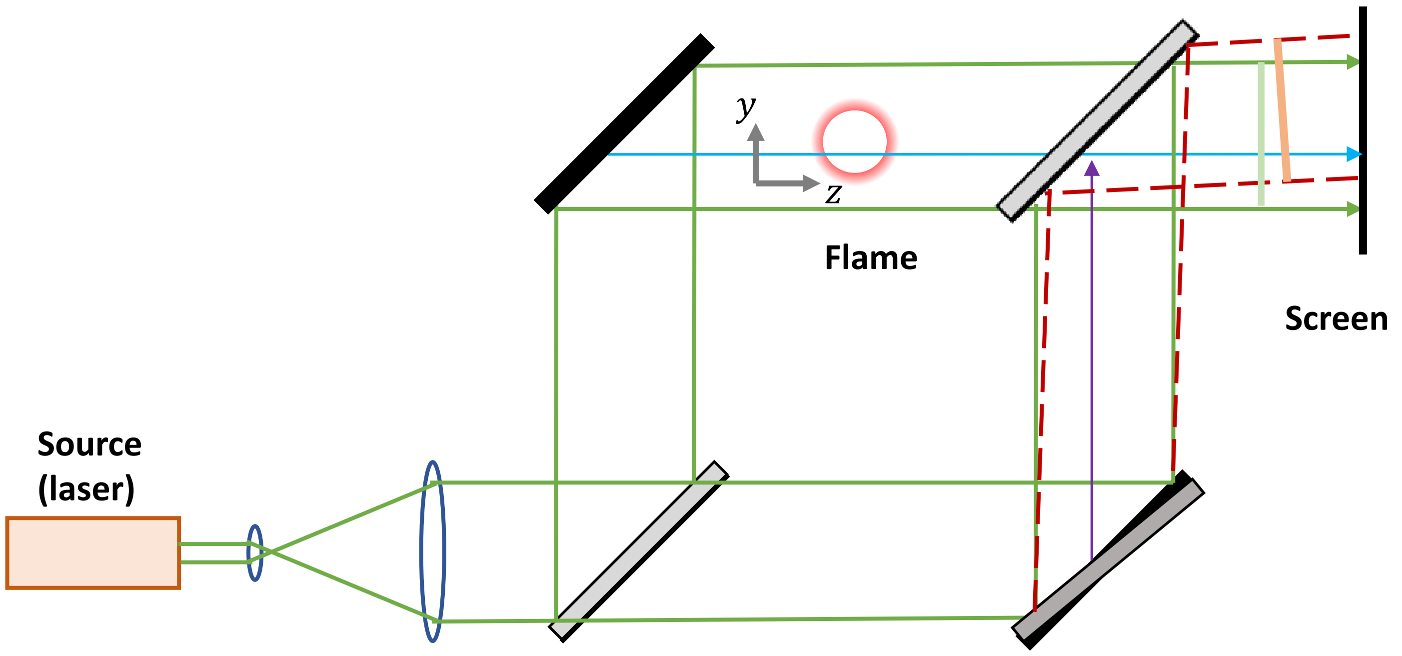


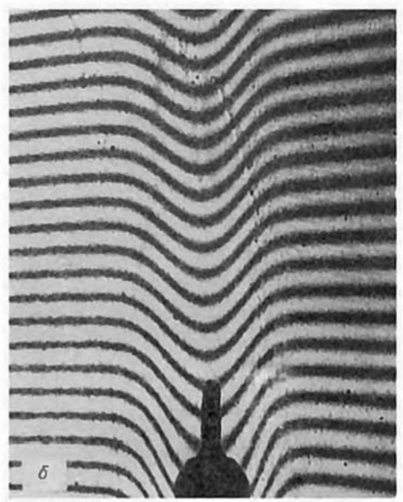

- One of the mirrors is rotated by a very small angle.
- Measuring and comparison waves propagate at a small angle and form an interference pattern of parallel fringes distanced by $d = \lambda/2 \cdot \sin(\alpha/2)$.
- When a flame is introduced, these fringes are bent.
- Local shift of fringe pattern, $\Delta x$, can be expressed in units of inter-fringe distance, *d,* (without the flame): $\Delta x = nd$
- Then the local phase shift introduced by flame is $\Delta\varphi = 2\pi n$
- Bad quality optics can be used, as the flame interferogram is compared with the fringe pattern which already contains distortions caused by the optics.

# Interferometry of burning Mg particle

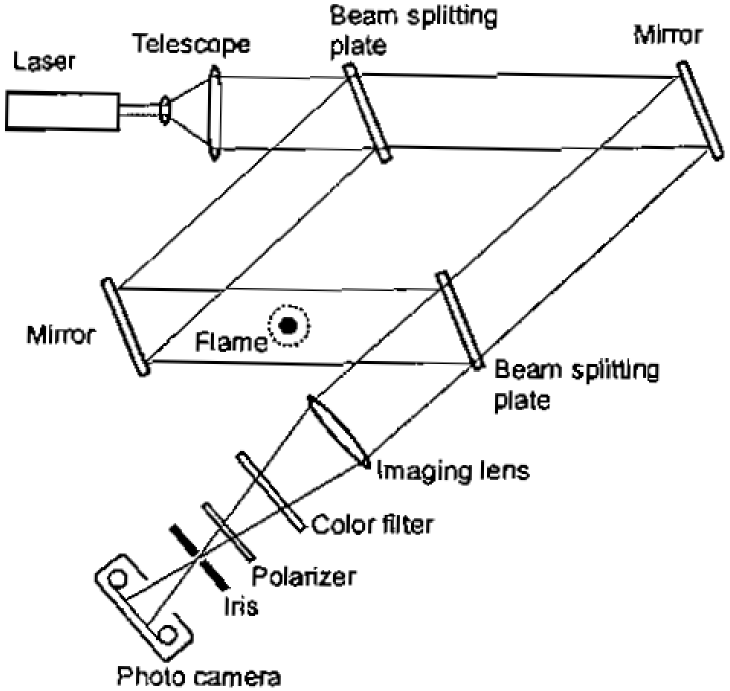


(Y. Shoshin, I. Altman, 2002)

- 1-3 mm dia. Mg particles were used.
- A narrow dense MgO condensation zone is formed around the burning Mg particle.
- Oxide nano-particle scatter light reducing the beam intensity up to 50 times.
- 30/70 % beam splitters are used to make the initial intensity ratio of ~5 between the two beams and to provide a good contrast over the whole interferogram.

# Interferometry of burning Mg particle. Some results.

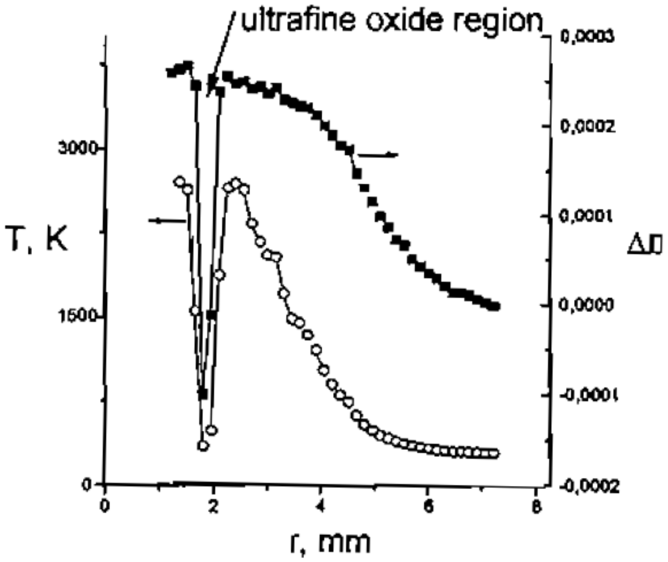


Radial profiles of local refractive index and formally calculated temperature. Initial particle radius 0.9 mm..

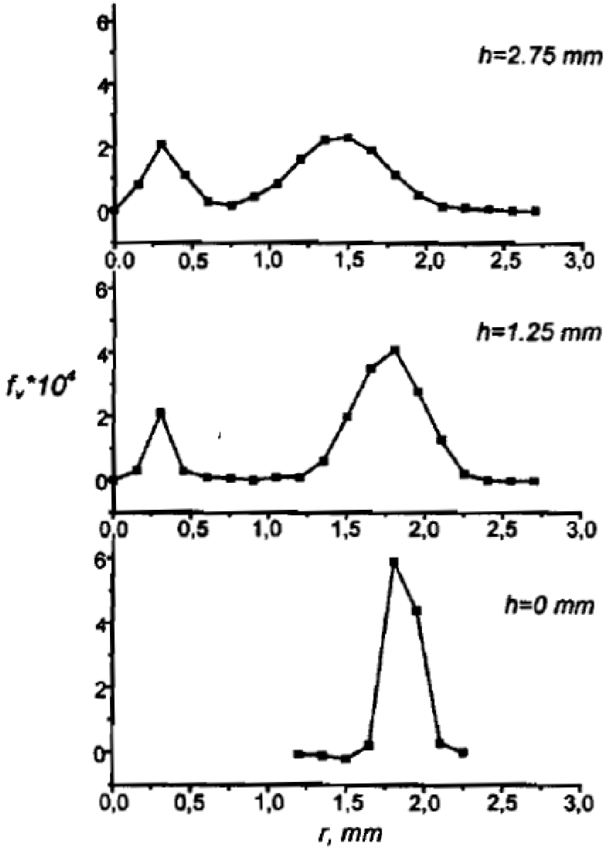


Restored by the interferogram ultrafine oxide volume fraction profiles at different heights from the burning particle center. Initial particle radius 0.9 mm.

- Nano-particles contribute into the local refraction index proportionally to their local volume fraction, $f_v$:

$$\Delta n = \frac{3}{2} f_v \frac{\varepsilon - 1}{\varepsilon + 2}$$ (L.Landau, E.Lifshitz, 1984)

- The contribution of nano-particles can be determined using extrapolation of the gas refraction index into the condensation zone.
- Temperature in the condensation zone can be determined by the extrapolation of the gas temperature.
- If radiation power is measured, emissivity on nano-oxide can be determined (It turned out to be 3 orders of magnitude higher than one predicted by $Al_2O_3$ conductivity at that temperature).

(Y. Shoshin, I. Altman, 2002)

# Holographic interferometry. How hologram works.

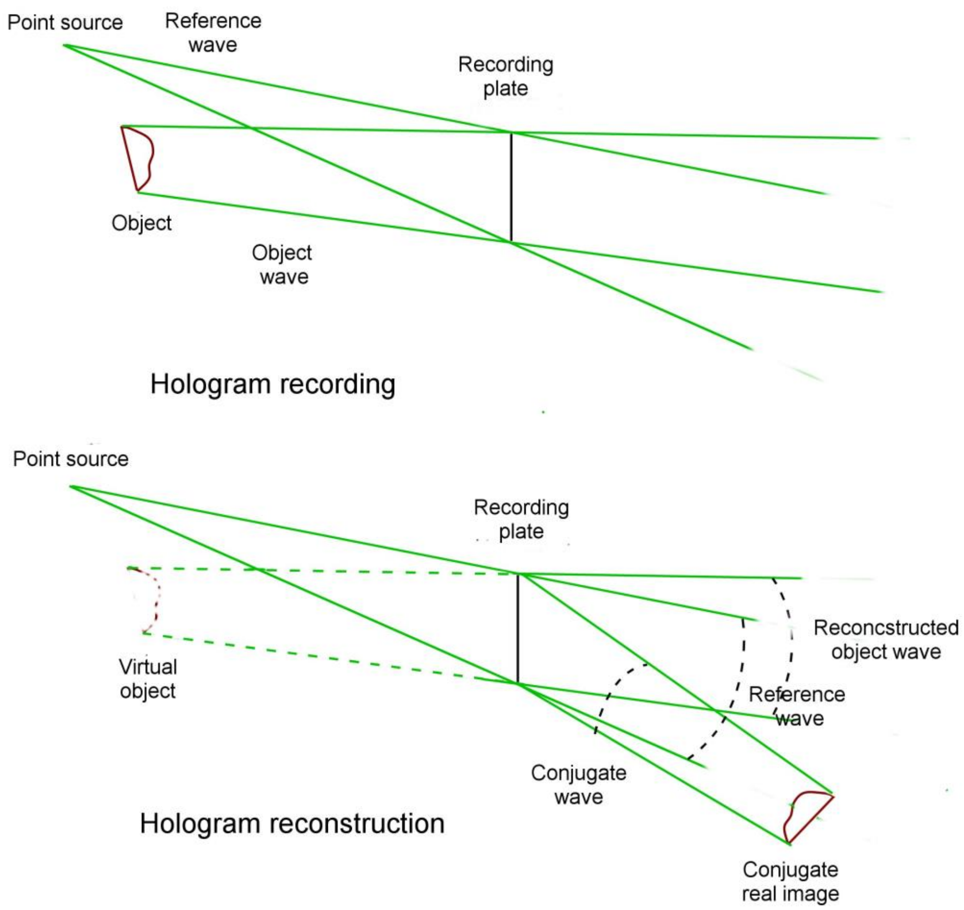


- Interference pattern produced by the reference and object wave is recorded on a photographic plate.
- Plate is developed and illuminated by a copy of the reference wave.
- A copy of the object wave is reconstructed behind the plate.
- The observer sees light, not the object.
- Can qualitatively be understood from Huygens's principle. Dark and light points on the plate act as coherent secondary sources, which interfere resulting in the reconstructed wave.

# Holographic interferometry. How interferogram is recorded.

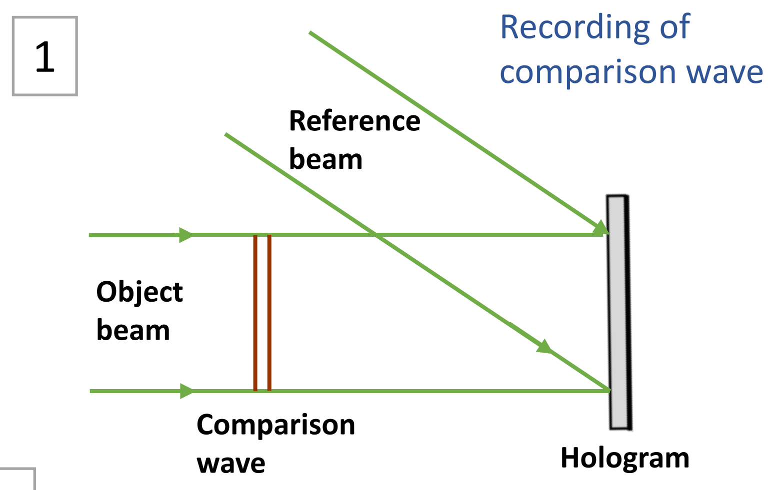


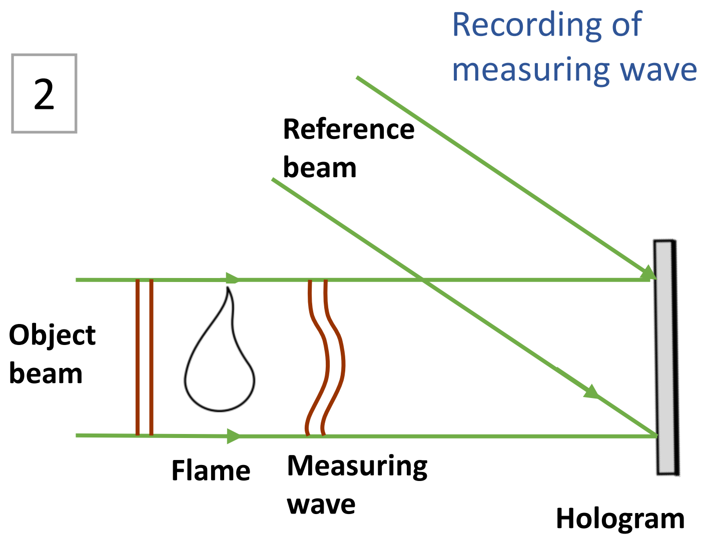


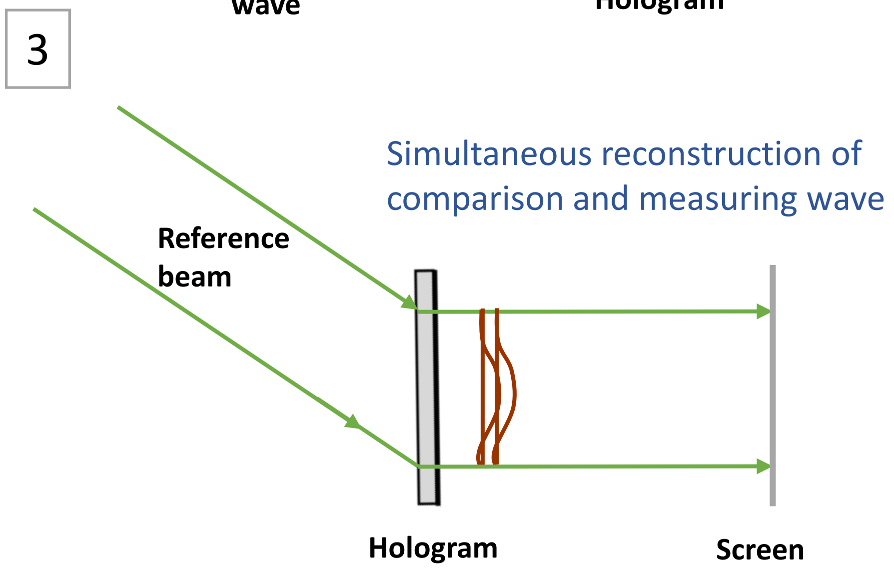


- Two holograms are recorded on the same photo plate:
    1) Hologram of undistorted (by flame) object beam (comparison wave).
    2) Hologram of distorted object beam (measuring wave).
- When the holographic plate is illuminated by the reconstructing beam, both waves are reconstructed and produce the interference pattern
- Low-quality optics or windows can be used.
- A comparison wave does not have to be flat. Even an interferogram of flame burning in a tube can be produced.

# Measurements of temperature field in Bunsen flames of metal suspensions with holographic interferometry.

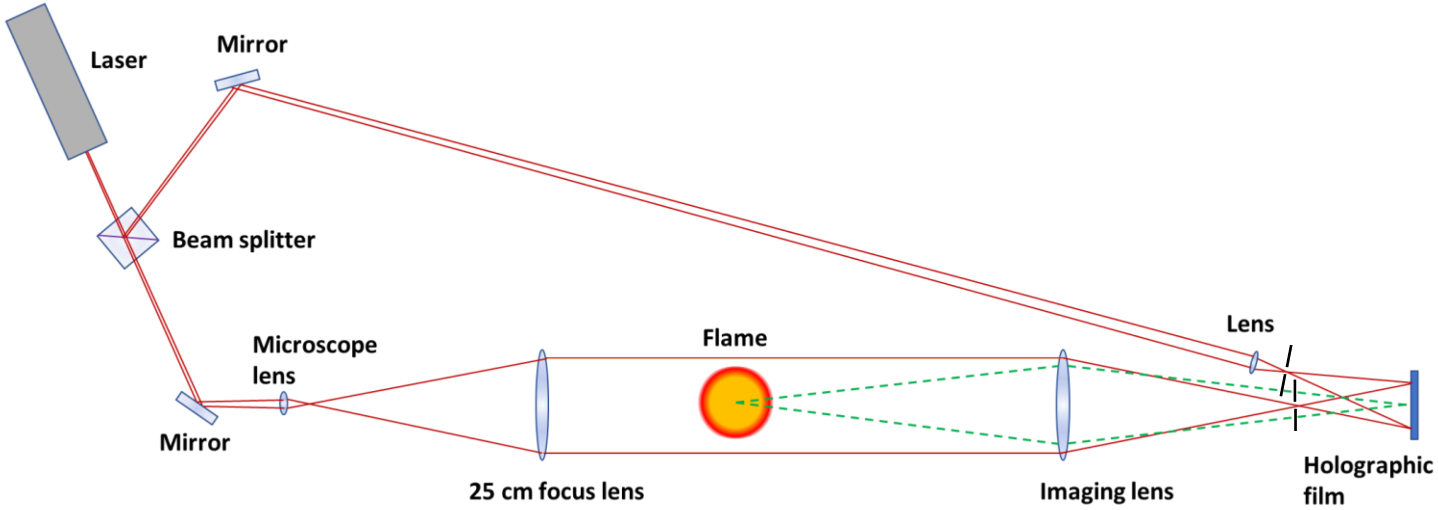


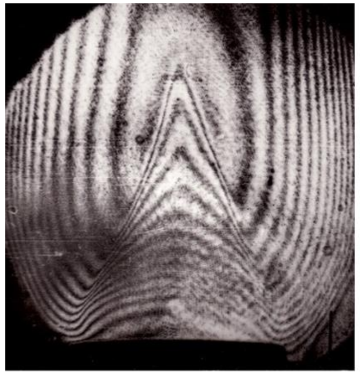

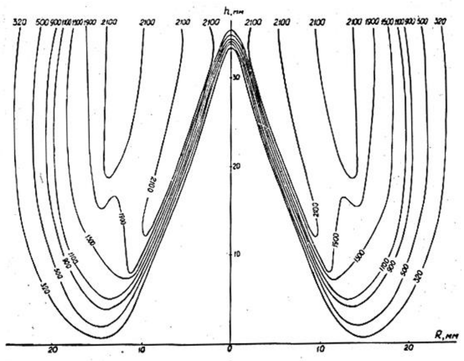

- The importance of radiation heat transfer for small laboratory flames of metal suspensions has been a topic for discussion for many years.
- In some works, it was assumed to be the main mechanism of flame propagation (flames propagating in tubes).
- It is difficult to measure gas phase temperature in such flames by other methods.
- Interferometric measurements showed that radiation heat transfer plays no role in the mechanism of small-scale flame propagation in metal suspensions

(S. Goroshin ,Y. Shoshin, 1991)

# Digital holographic interferometry.
# Why it is used only by “holographic” researchers, but not by “combustion” ones?

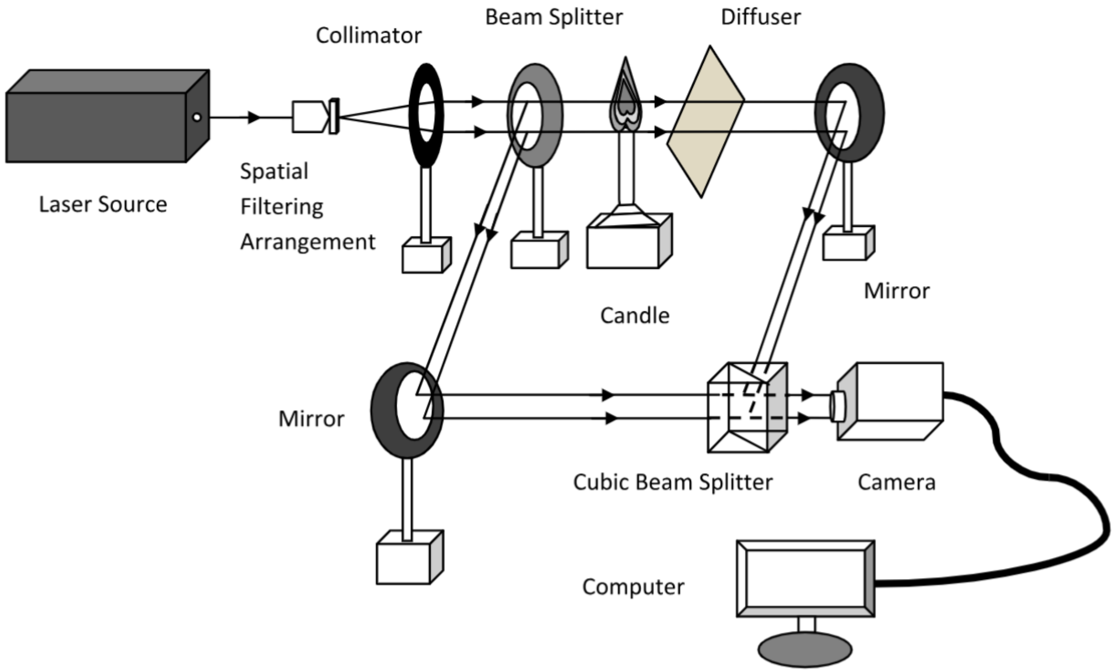


N. Jabeen and A. K. Nirala

- **Instead of a holographic photo plate, a CCD camera sensor is used.**
  - Reference and comparison holograms are registered on two separate frames.

**Advantages:**

- Film development, physical hologram reconstruction, and making again photos of the reconstructed interferogram are eliminated.
- Comparison and measuring waves and, therefore, the interferogram can be reconstructed by pushing a button provided you have the appropriate software.

**Drawbacks:**

- Camera sensor resolution is still much lower than the resolution of a holographic plate. Only very small angles between the reference and signal waves are possible.
- No free or commercial software is available. No printers exist to print a hologram with sufficient resolution to physically restore it.
- **One has to write his software based on scary equations to reconstruct holograms.**
- **Can digital reconstruction of light waves be avoided? Yes.**

# Holographic interferogram as (invisible) Moire pattern.

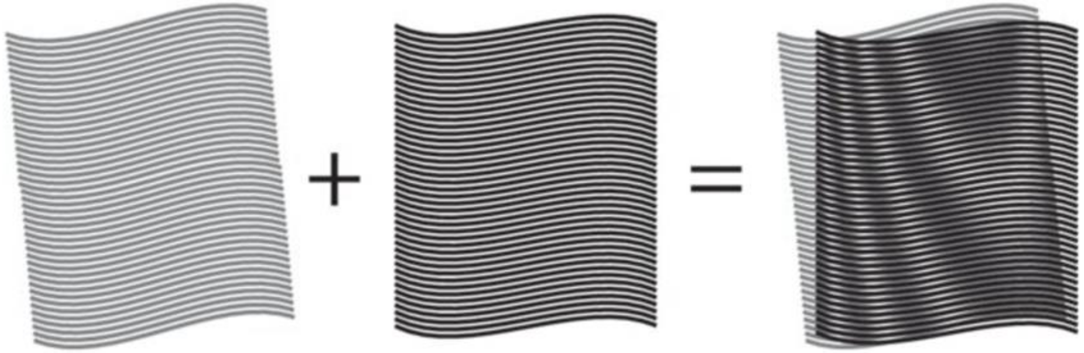

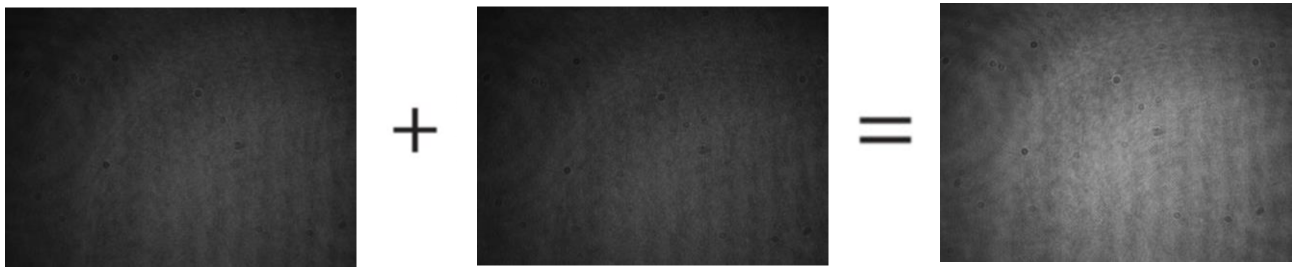

**Comparison hologram** **Measuring hologram** **Sum**

- Moire pattern occurs when a set of near-periodic lines is superposed onto another set.
- Usually leads to visible low spatial frequency light intensity modulations.
- In holographic interferometry, comparison and measuring holograms are, actually, sets of near-periodic fringes. When they are superimposed (sum of two holograms), the Moire pattern should occur.
- But it is not visible because of the sinusoidal modulation:

$$[1+\sin(x+\varphi_1)]+[1+\sin(x+\varphi_2)]=2+\sin(x+\varphi_3)$$

- Because of the sinusoidal modulation, the average value of the right side is constant (=2).

# Digital holographic interferometry of camping stove flame.

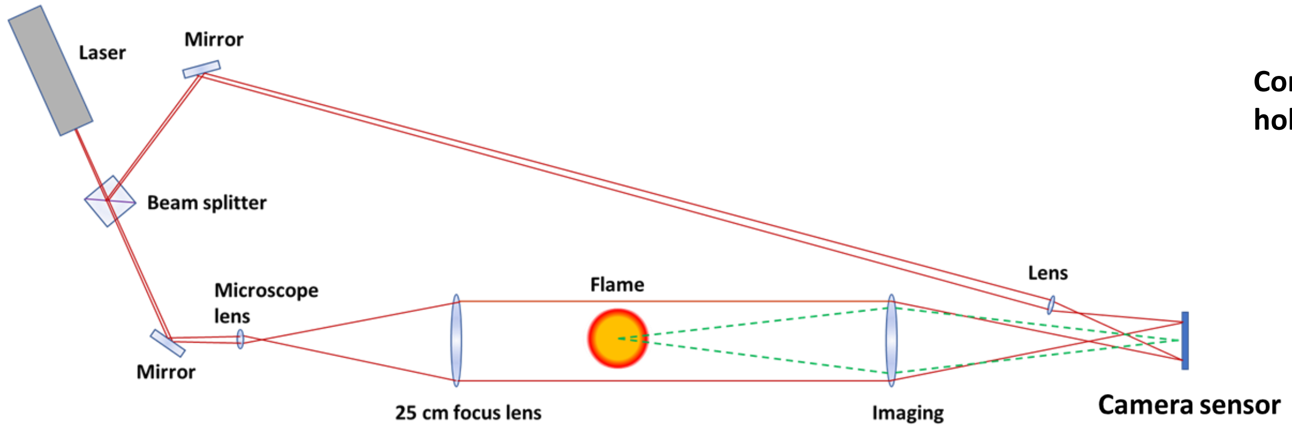


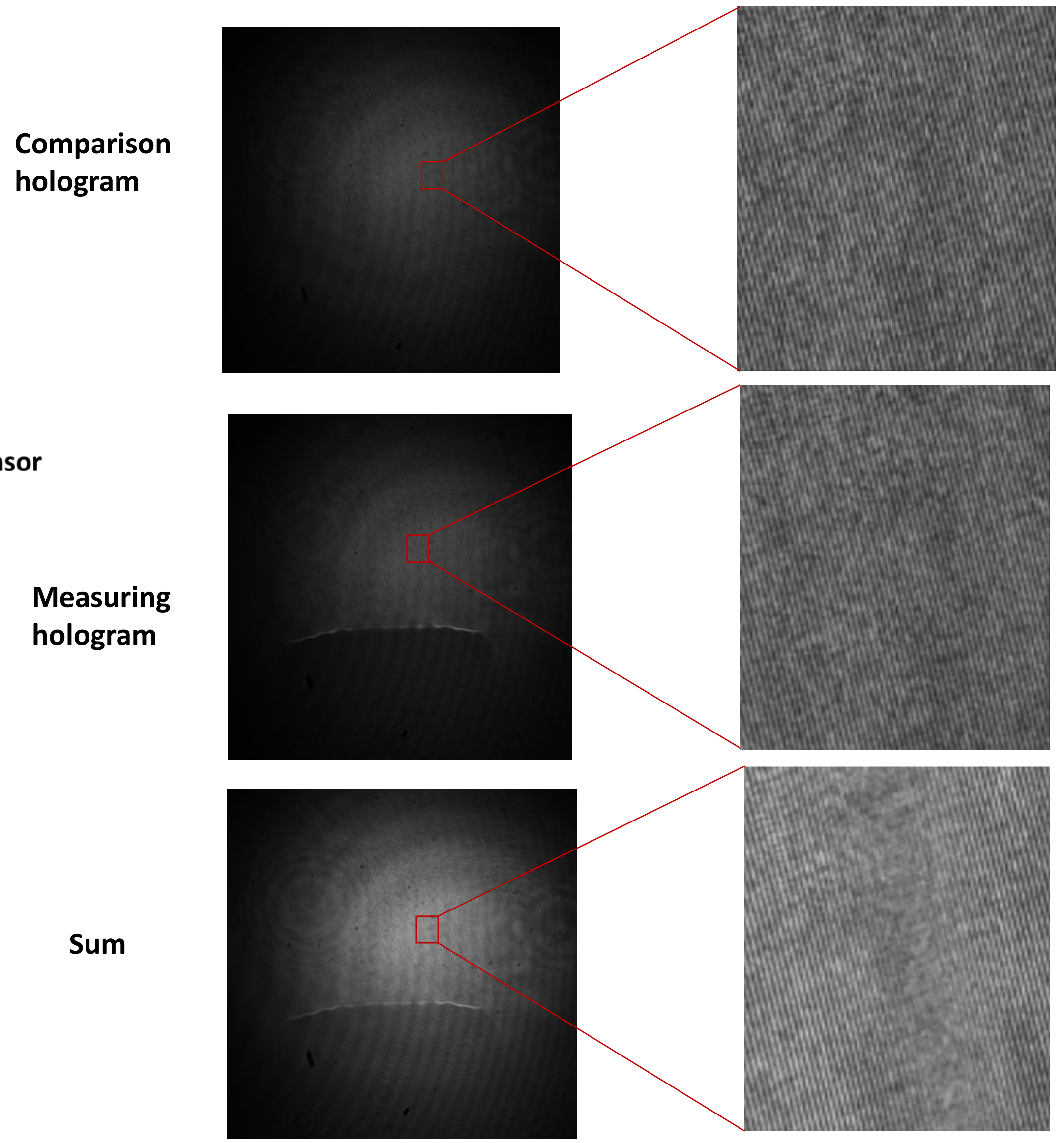


- The sum of the two holograms contains an interferogram "coded" by the local contrast of a high spatial frequency pattern.
- As the flame location was focused onto the sensor, the "coded" focused interferogram is located directly in the sensor plane.
- If there is a way to visualize this "coded" image, then there is no need for digital interferogram reconstruction.

# Digital holographic interferometry without image reconstruction.

**Comparison hologram**

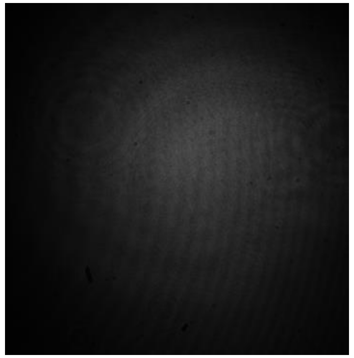

**Measuring hologram**

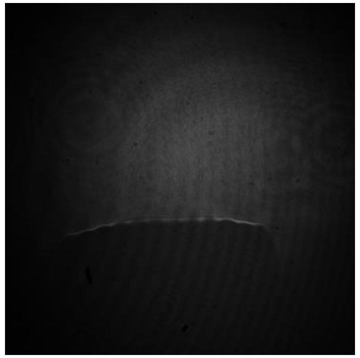

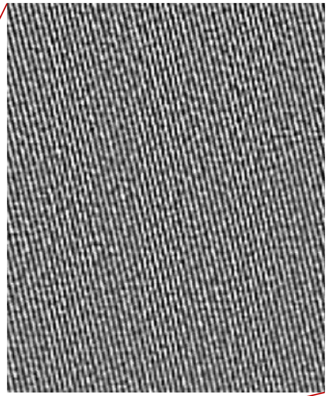

A better way: using the "standard deviation function" for the two filtered images.

The intensity of each pixel scales with deviations of the pixel intensity from their average value.

It is small where fringes coincide and large where fringes are in opposite phases.

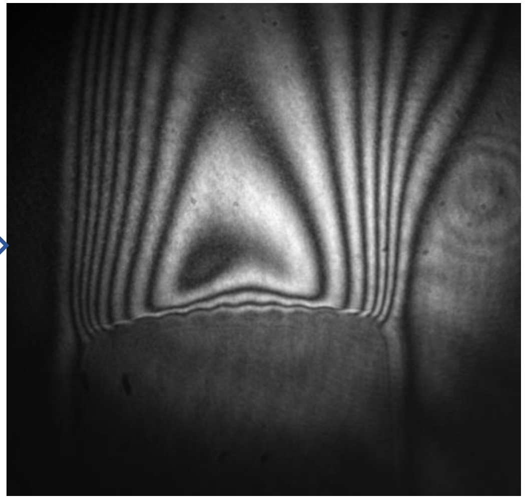

Bandpass filter applied

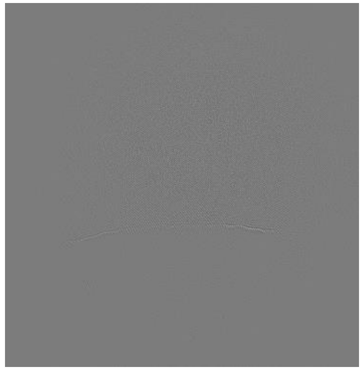

+

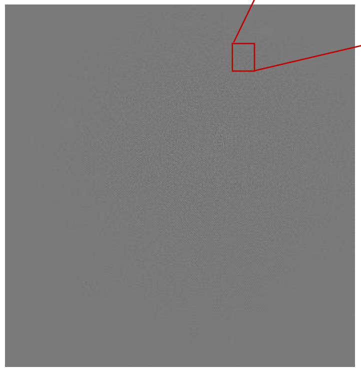

=

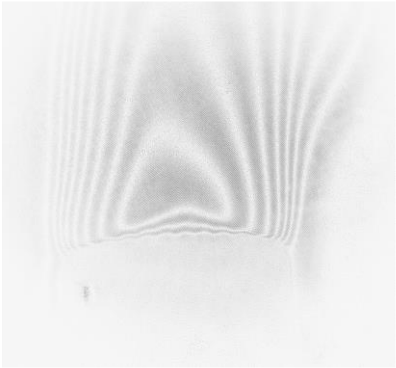

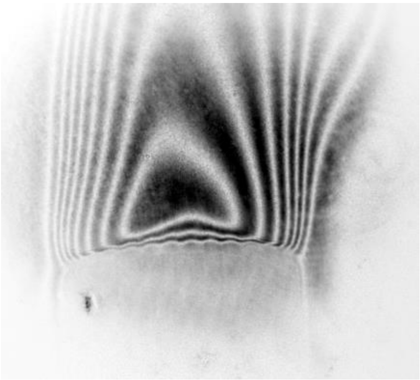

Contrast enhanced and filter applied.

# Flame radiation loss measurements. Selection of a photodetector.

**Main detector selection criteria**:

1. Flat response over the whole spectral range where flame radiates noticeably.
2. High sensitivity.
3. Sufficiently large sensor area, so that a precision aperture can be installed in front of it.

- Some thermopile and pyroelectric photodetectors are the right choice.
- Pyroelectric detectors, in general, a more sensitive (from ~100 nW) than thermopile ones (from ~10 µW), but require modulation light (chopper).
- Similar response times (seconds).
- **Thermopile detector allows measuring the total energy radiated during a finite period, regardless of its duration.**

**Example: Thorlabs S401C thermopile detector.**

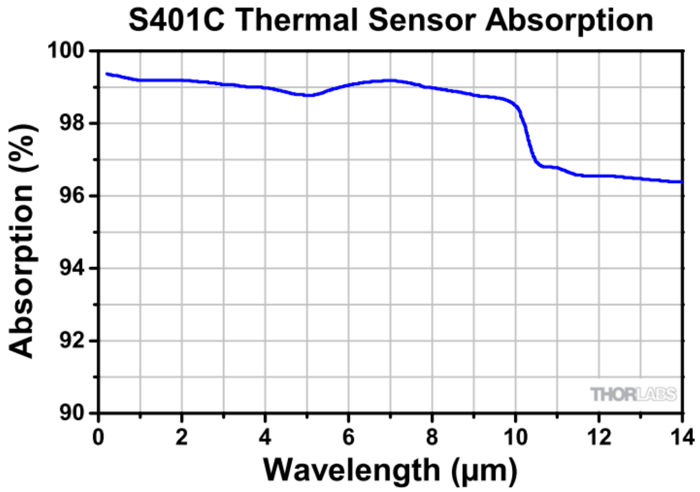


- Wavelength Range 190 nm - 20 µm
- Optical Power Working Range 10 µW – 1 W
- Measurement Uncertainty ±3% @ 1064 nm; ±5% @ 190 nm – 10.6 µm
- Response Time 1.1 s
- Input Aperture Ø10 mm

# Flame radiation loss measurements. Thermopile detector.

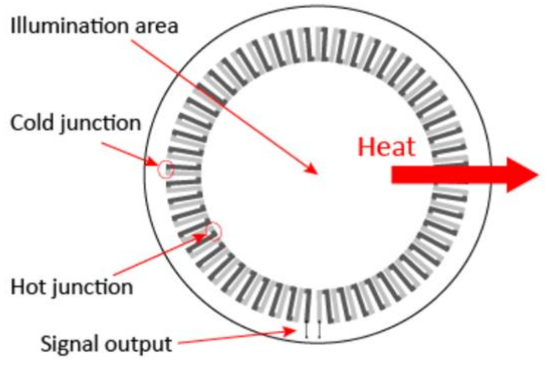


Short radiation pulse

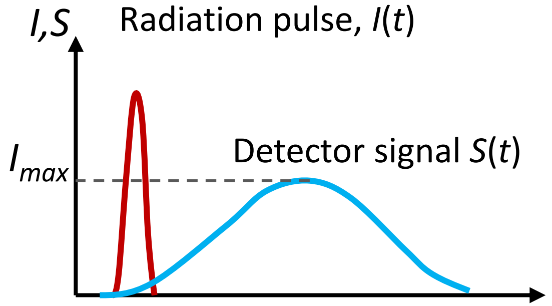


*$I_{max}$ ~ Pulse energy*

- **For continuous radiation sources**, the signal becomes proportional to the radiation power after the response time.
- **For short radiation pulse** (<< response time), the peak signal is proportional to the energy of the pulse.
- **Can measurements be performed in between these cases?** Manufacturers say “no”…

Radiation of any finite duration and arbitrary temporal profile

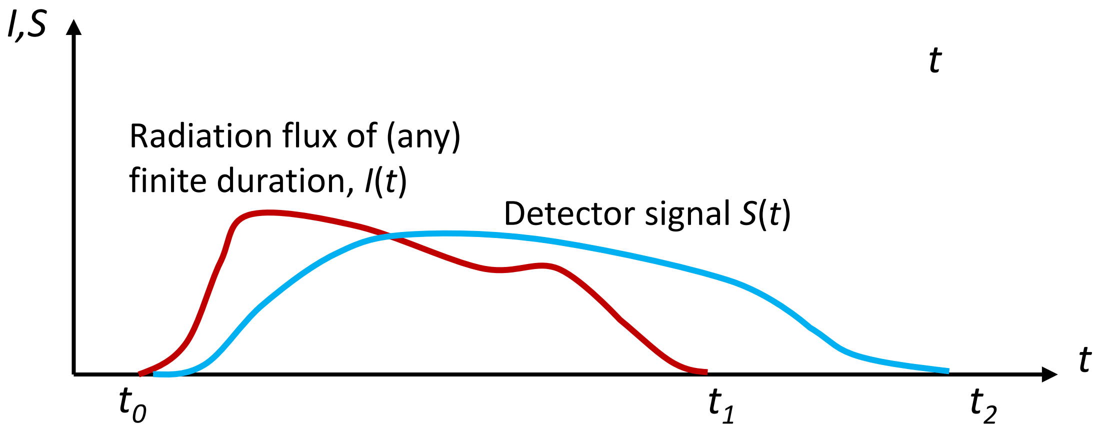


- The signal is proportional to the temperature difference between the illuminated area and the cold periphery area, e.g. to the heat flux.
- All the heat received by radiation is eventually transferred to the periphery $\Longrightarrow$

$$E_R = \int_{t_0}^{t_1} I(t)dt = k \cdot \int_{t_0}^{t_2} S(t)dt$$

# Integral radiation loss measurements (over the whole flame).

- Most laboratory flames are optically thin.
- At large distances, such a flame can be treated as an isotropic point source.
- This holds if some external structure, e.g. burner, blocks some radiation unless it reflects or scatters flame radiation toward the photodetector

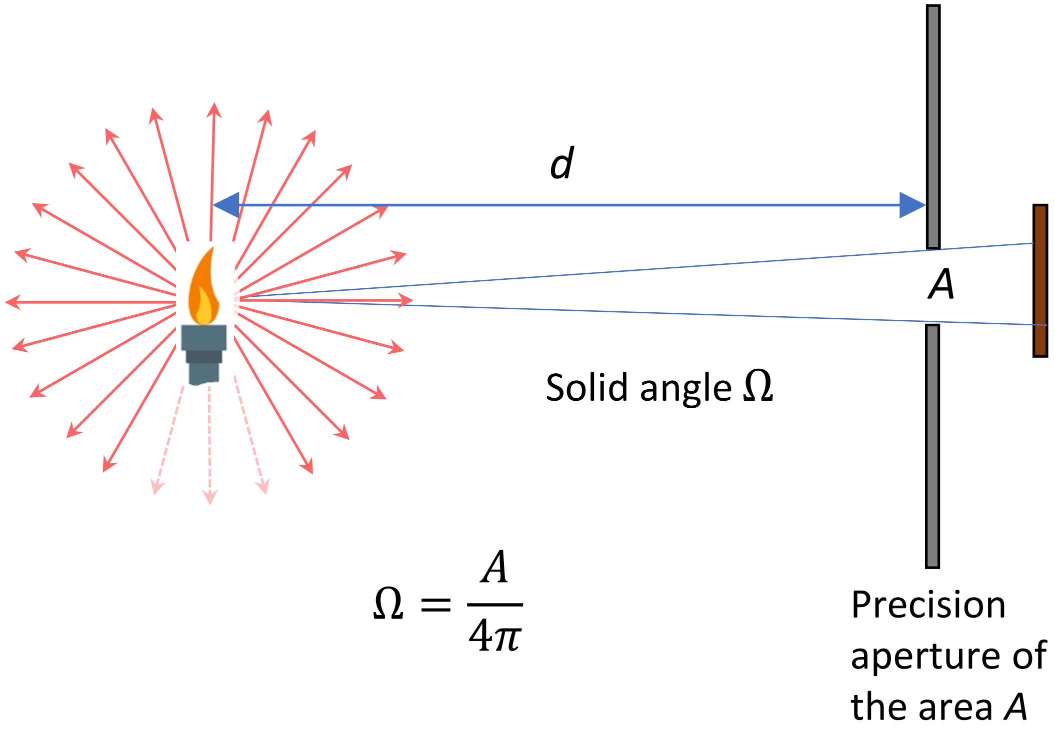


$$\Omega = \frac{A}{4\pi}$$

- Steady state flame, the total radiation power:
- $P_R = k \cdot S \cdot \frac{4\pi}{\Omega}$ (after the response time).
- Finite combustion time, e.g. single particle combustion, total radiated energy:
- $E_R = k\frac{4\pi}{\Omega} \cdot \int_{t_0}^{t_2} S(t)dt$

# Radiation loss measurements per unit are of a flame front.

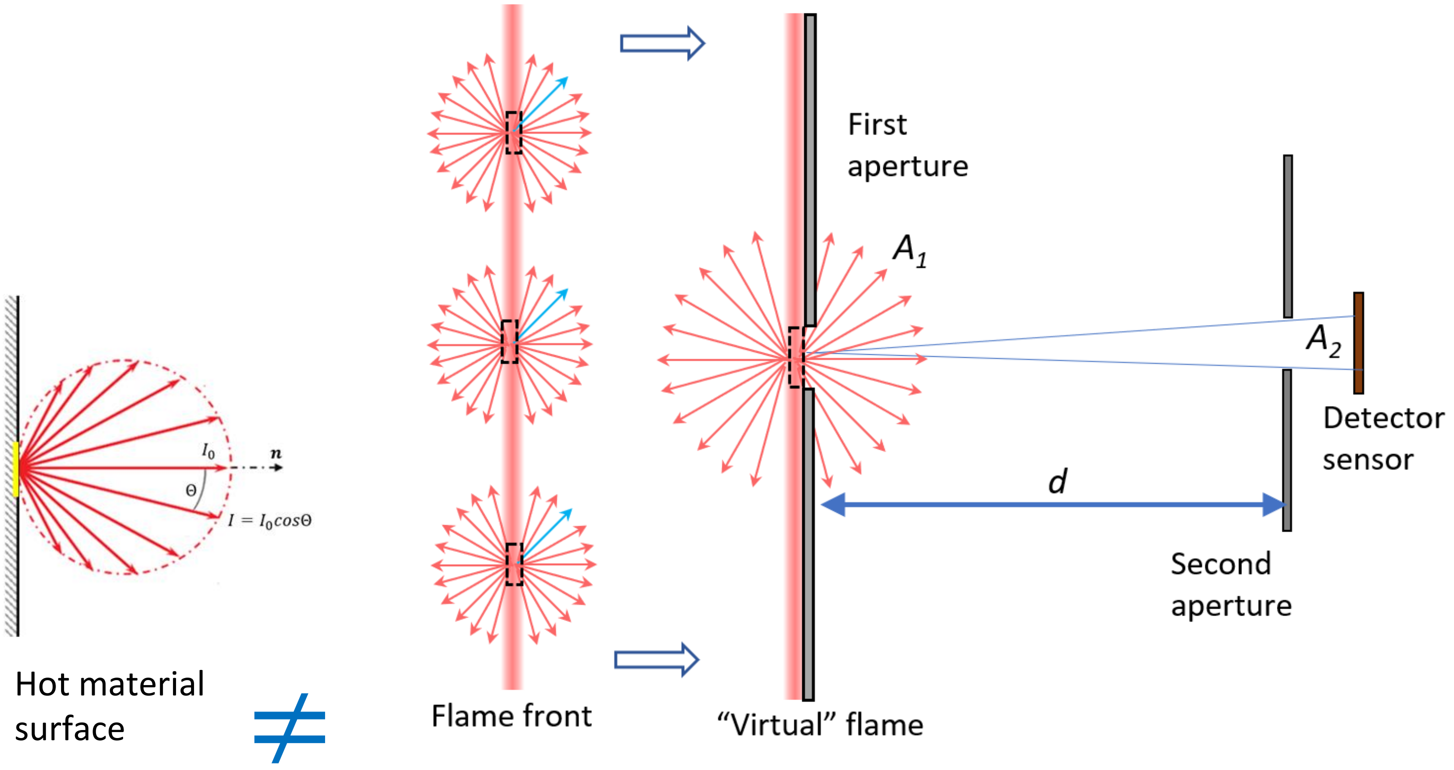


- Flame front radiates differently than a hot material surface.
- The value of interest: total power lost by radiation per unit of flame surface, $q = \frac{\delta P}{\delta A}$
- Radiation through a hole in a screen, does not depend on the distance to the flame front :
    - We can assume that the flame front is located directly in the hole plane.
- A small flame segment radiates isotopically.
- Total radiation power received by the detector: $W = q \cdot A_1 \cdot \frac{\Omega}{4\pi}$ with $\Omega = \frac{A_2}{d}$.

Thus, $W = q \cdot \frac{A_1^2 \cdot A_2^2}{4\pi}$ and

$$q = \frac{4\pi \cdot W}{A_1^2 \cdot A_2^2}$$

# Laser attenuation measurements for solid/liquid aerosols fuel fraction.

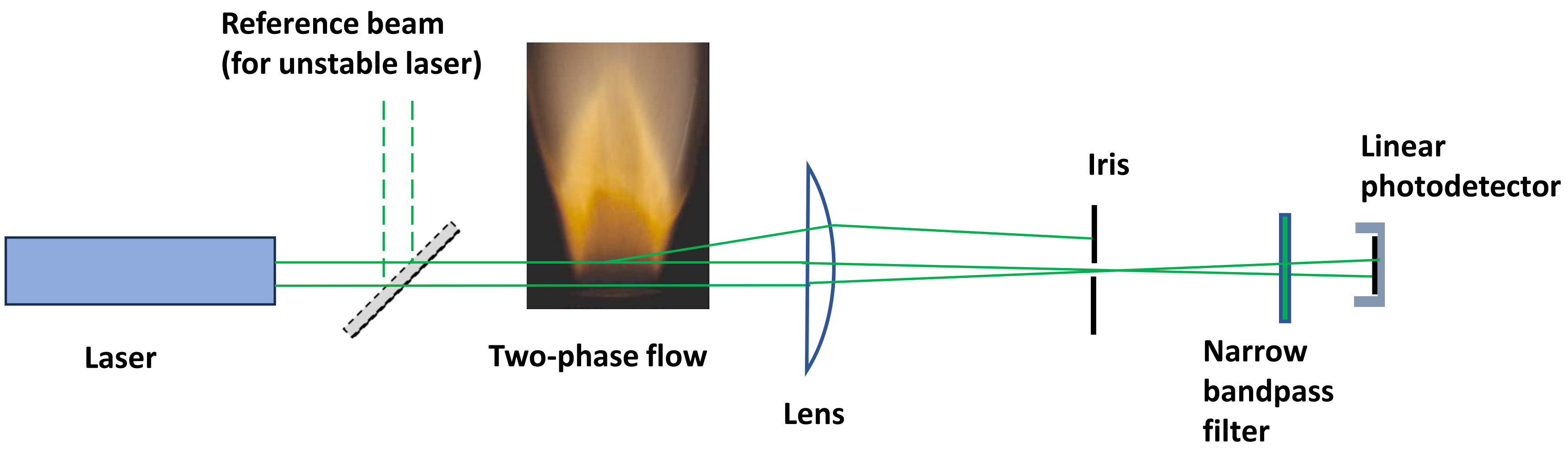


- Pinhole is necessary (lens + iris). A bandpass filter does not remove scattered light.
- Photodetector sensor diameter should be much larger than the diameter of the laser spot. Otherwise, small beam deviations, e.g. due to vibrations, will result in signal variations.

# In situ particle size measurement. Common approach.

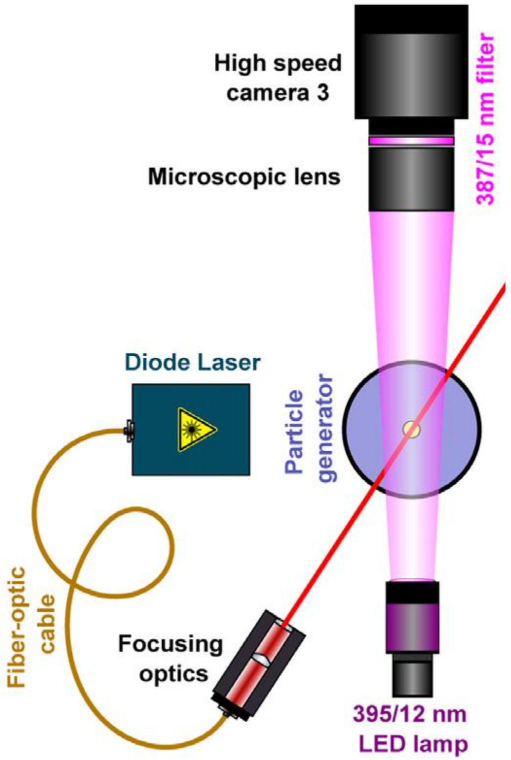


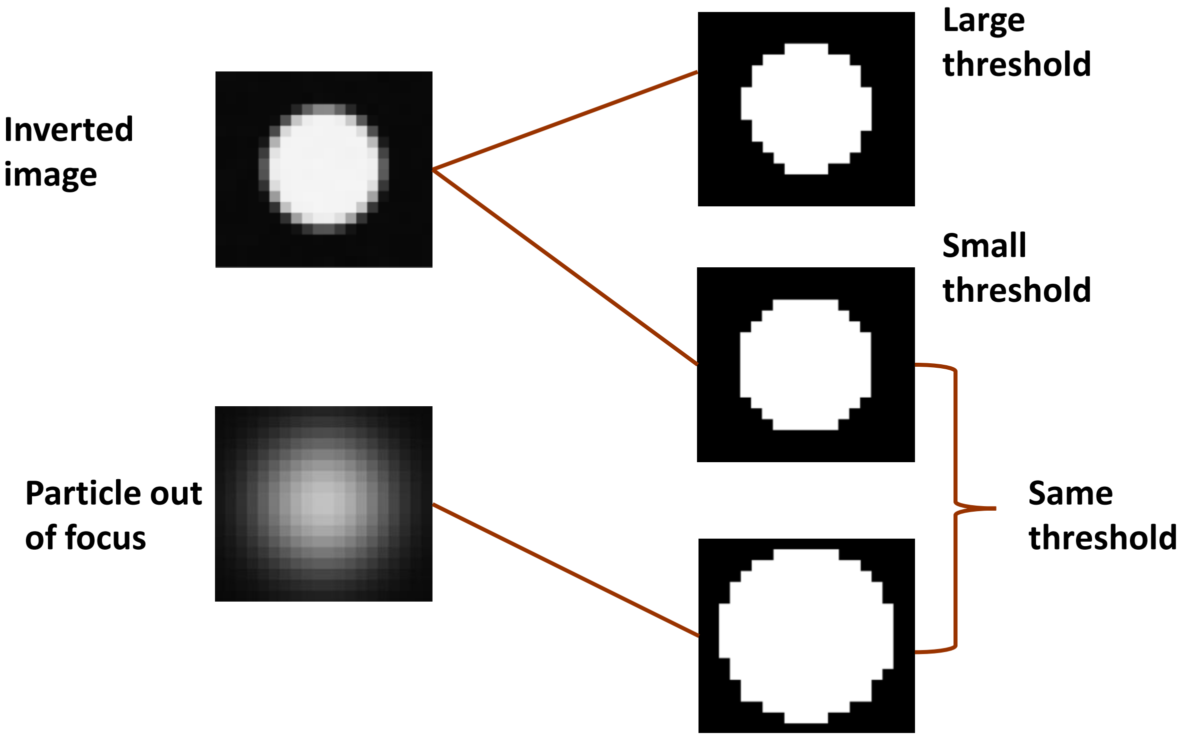


- Image is inverted.
- Background subtracted (optionally).
- An arbitrary threshold is set to detect particle edge contour.
- Particle size is determined from the area inside the contour.
    - Result depends on the threshold value.
    - Quality of focusing affects the result.

# In situ particle size measurement. Light attenuation approach, background correction.

## Background subtraction

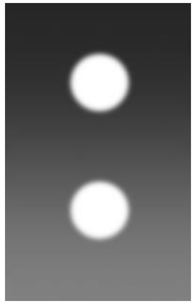

**Inverted original image**

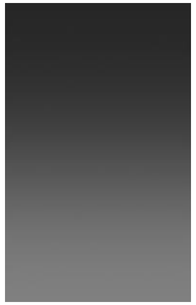

**Inverted background**

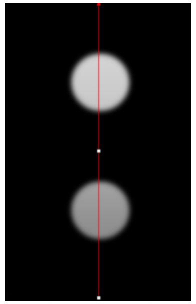

**Background subtracted**

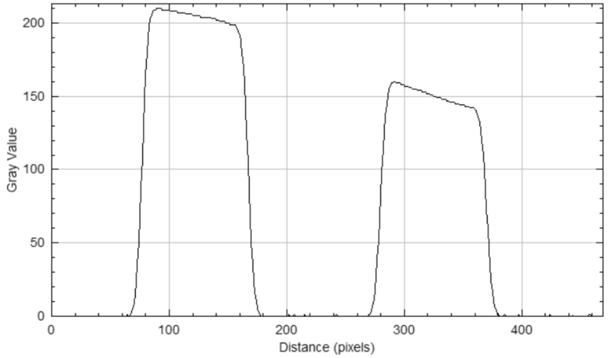


- For large particles $(d \gg \lambda)$, the total light attenuation integrated over the particle image is proportional to the particle projection area, regardless the quality of focusing.

## Division by background

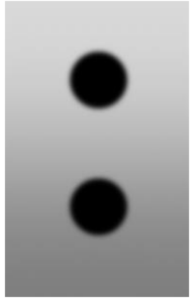

**Original image**

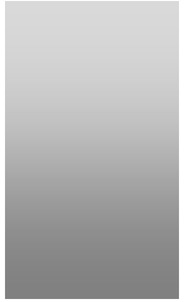

**Background**

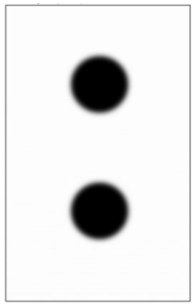

**Image divided by background**

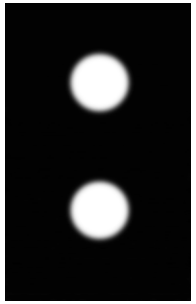

**Inverted background-corrected image**

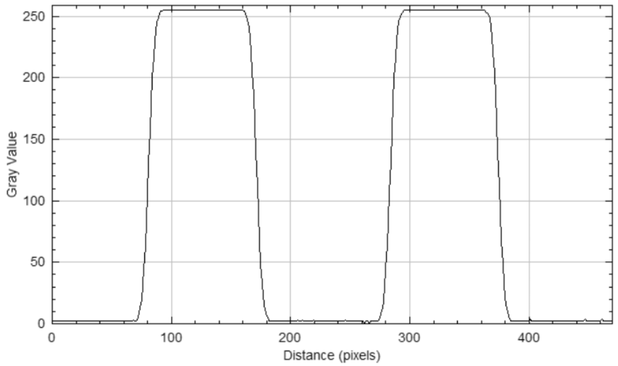

# In situ particle size measurement. Light attenuation approach: noise and integration area.

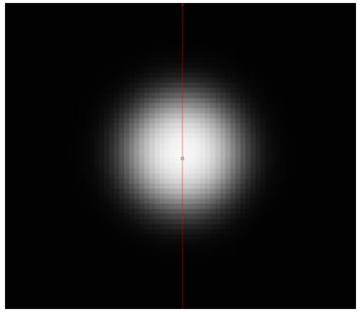

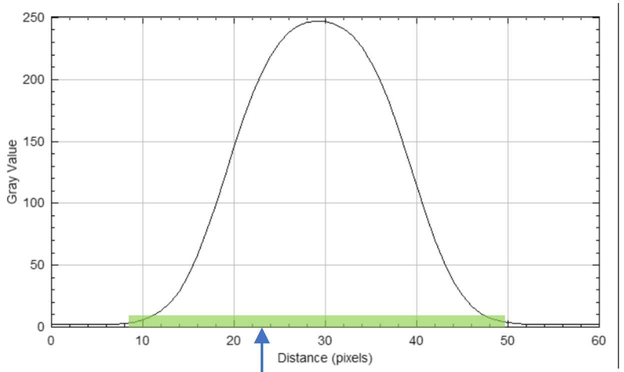


**Correct integration area**

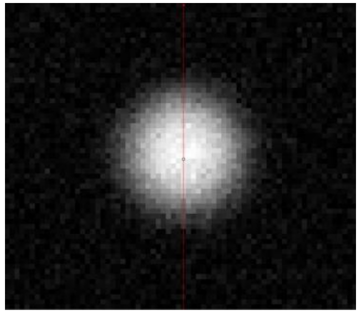

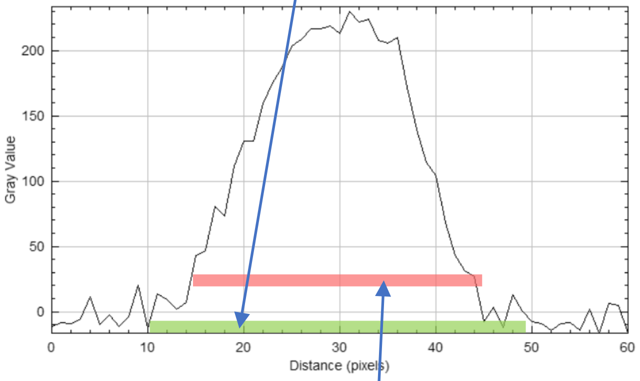


**Integration area defined by min. threshold for an image with noise.**

- Noise is present on the original and background-corrected image.
- Correction for background results in negative noise values for some pixels.
  - Do not use image formats with positive values only. Better use text files.
  - Do not delegate background correction to the camera.

- Noise affects min. threshold value. But there is a signal outside this threshold area.
- Integration area should be extended beyond the threshold area.

# Rayleigh scattering measurements in small confinements.

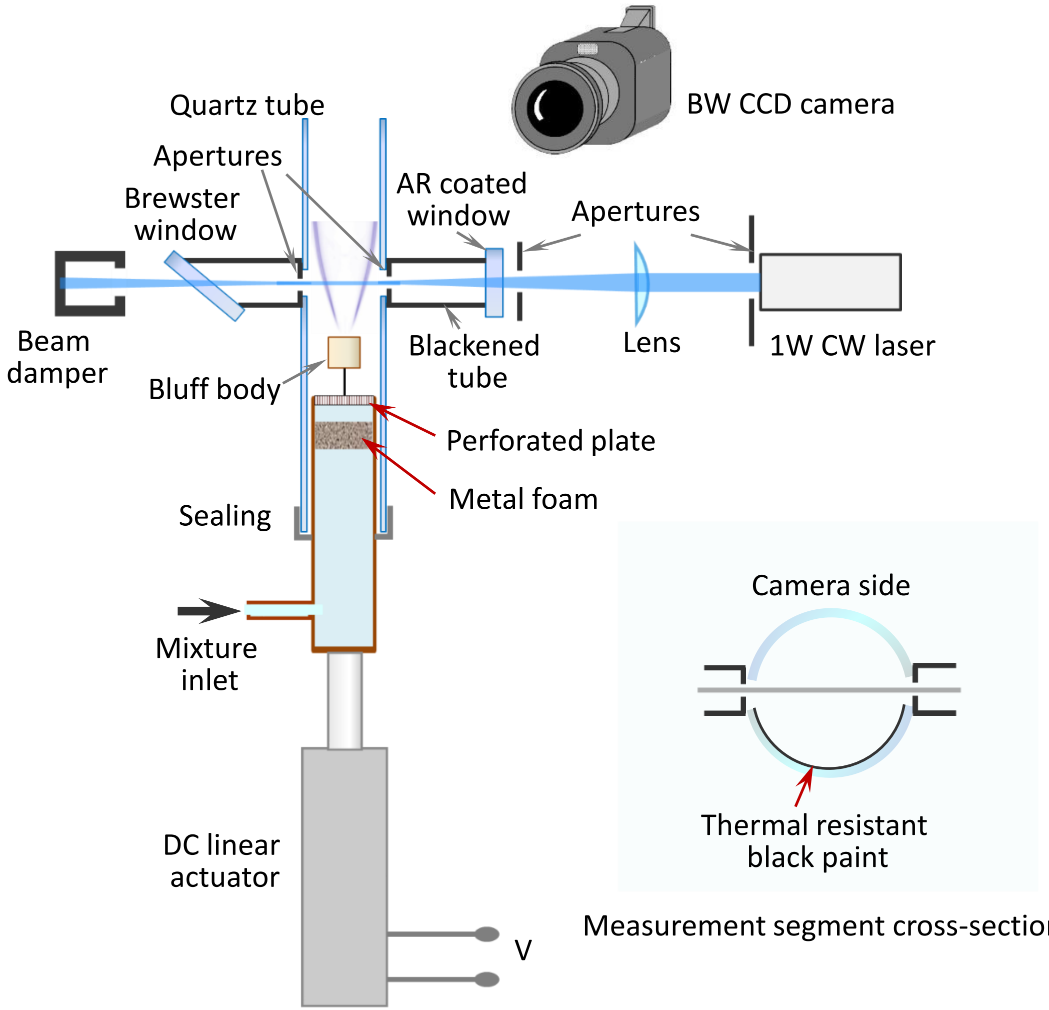


Measurement segment cross-section

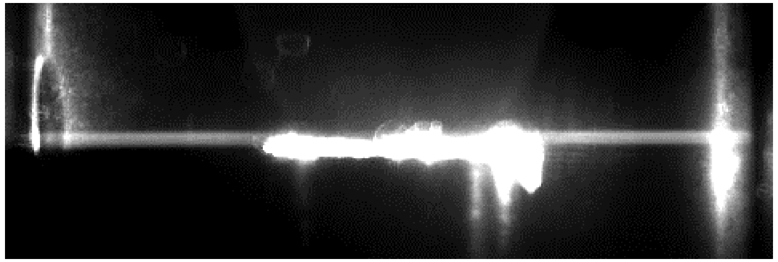

- 1 W blue diode laser ($\lambda$ = 0.45 µm).
- Line-wise measurements: high ratio signal to noise (scattering + flame radiation).
- Flame traverses the laser beam, camera records the signal.
- Signal integrated across the laser beam image.
- 2D temperature distribution recovered
- ~300 µm resolution.

# Rayleigh scattering. CH4-H2-air bluff body stabilized flames.

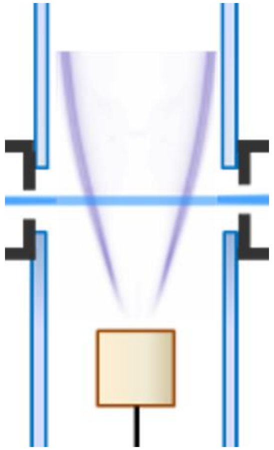

$$I_R \sim \sigma_{eff} \frac{1}{T}$$

$$\sigma_{eff} = \sum x_i \sigma_i$$

$$T_f = T_{cal} \frac{S_{cal}}{S_f} \frac{\sigma_f}{\sigma_{cal}}$$

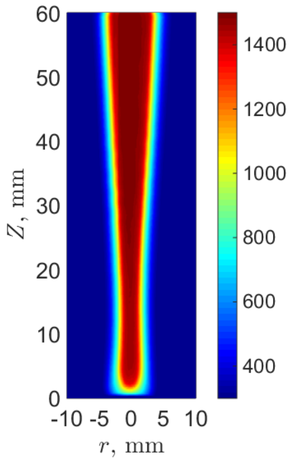


0.2 m/s 0% H2 Phi 0.521

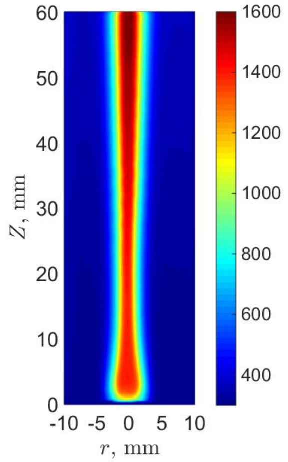


0.2 m/s 40% H2 Phi 0.323

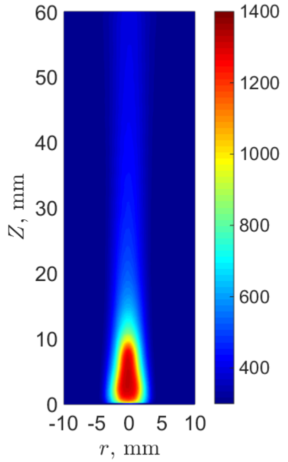


0.2 m/s 40% H2 Phi 0.316

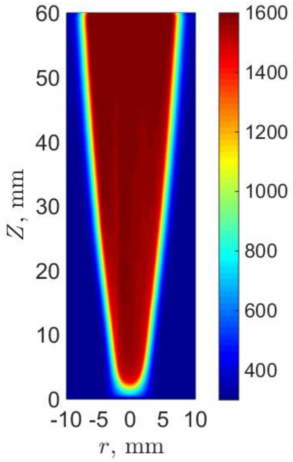


1 m/s 0% H2 Phi 0.54

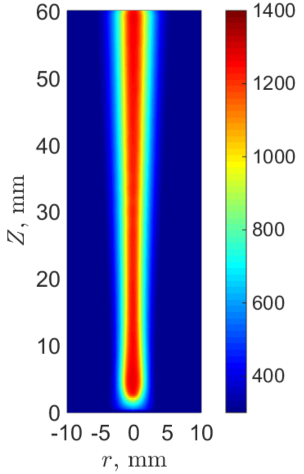


1 m/s 40% H2 Phi 0.357

# Rayleigh scattering. Flame caps and ball-like flame stabilized in a downward flow setup.

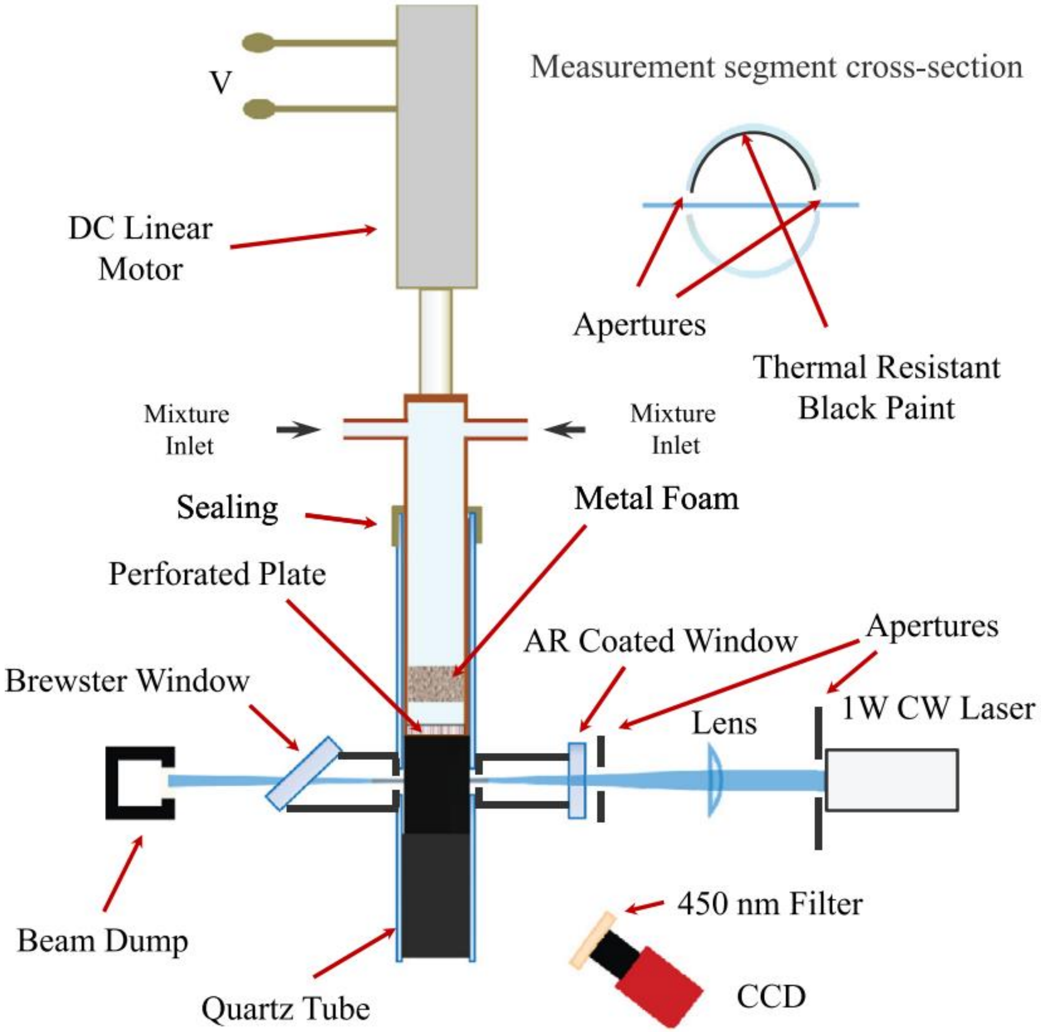


- Flames are stabilized in a tube in a uniform downward flow.
- Such flames are nearly equivalent to flame propagating upward in half-opened tubes when the downward flow velocity is equal to the flame propagation velocity.
- Ball-like flames and cup flames can be formed in Le < 1 mixtures.

(Z. Zhou, Y. Shoshin , F. E. Hernández-Pérez , J. A. van Oijen , L. P.H. de Goey, 2018)

# Rayleigh scattering. Flame caps and ball-like flame stabilized in downward flow setup. A

## Cup-like flames in a 30 mm dia. tube

**20%H2+80%CH4-air mixture**

(Z. Zhou, Y. Shoshin, F. E. Hernández-Pérez, J. A. van Oijen, L. P.H. de Goey, Comb. Flame 189 2018)

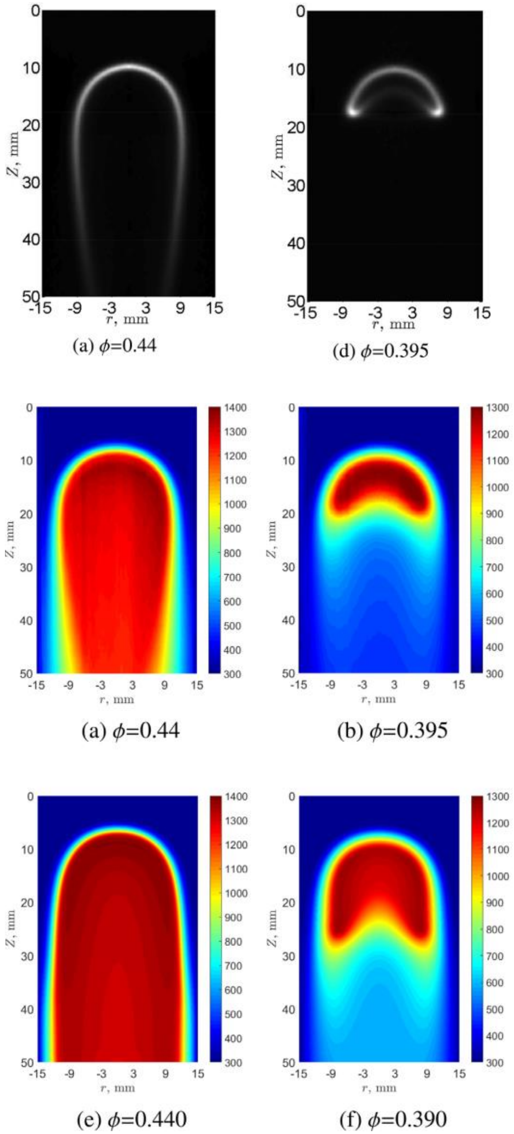


**Abel-inverted images**

**Measured temperature fields**

**Simulated temperature fields**

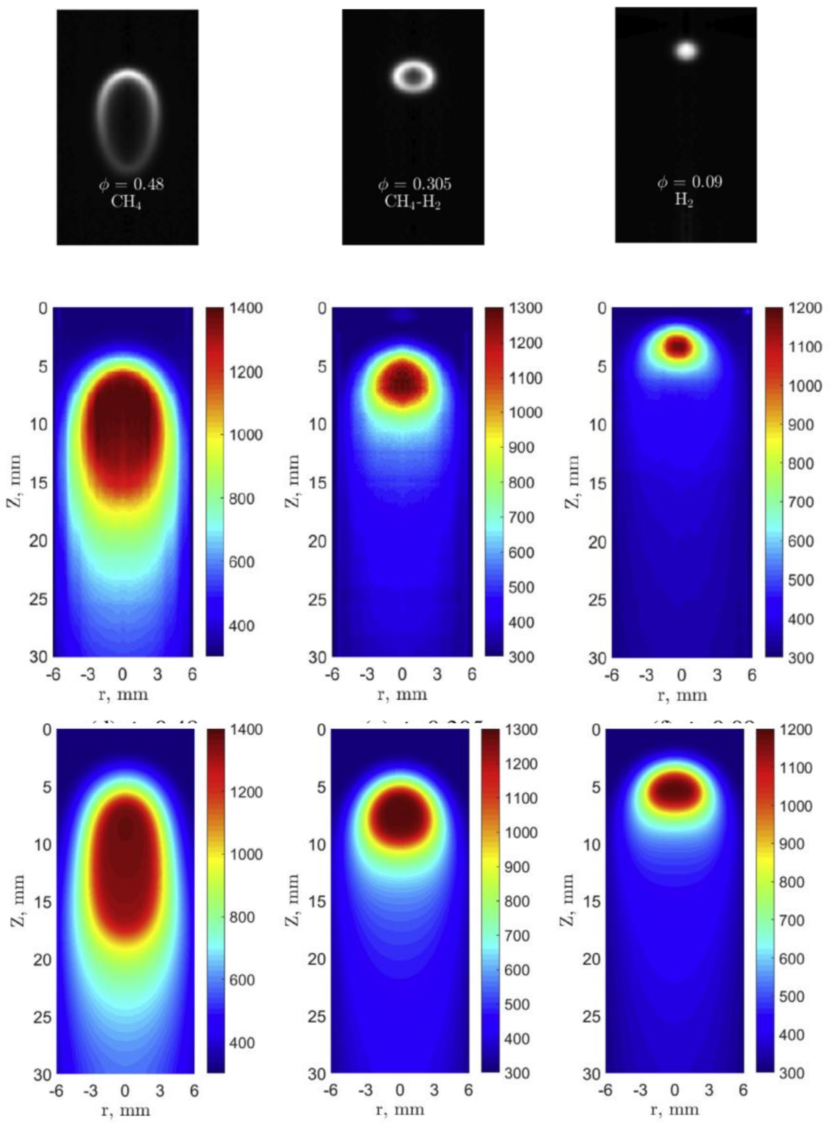


## Ball-like flames in a 12 mm dia. tube

**CH4–air (left), 40%H2+60%CH4–air (middle), and H2-air (right) mixtures**

(Z. Zhou, Y. Shoshin, F. E. Hernández-Pérez, J. A. van Oijen, L. P.H. de Goey, Comb. Flame 188, 2018)

# Color camera pyrometry of dust flames – problems.

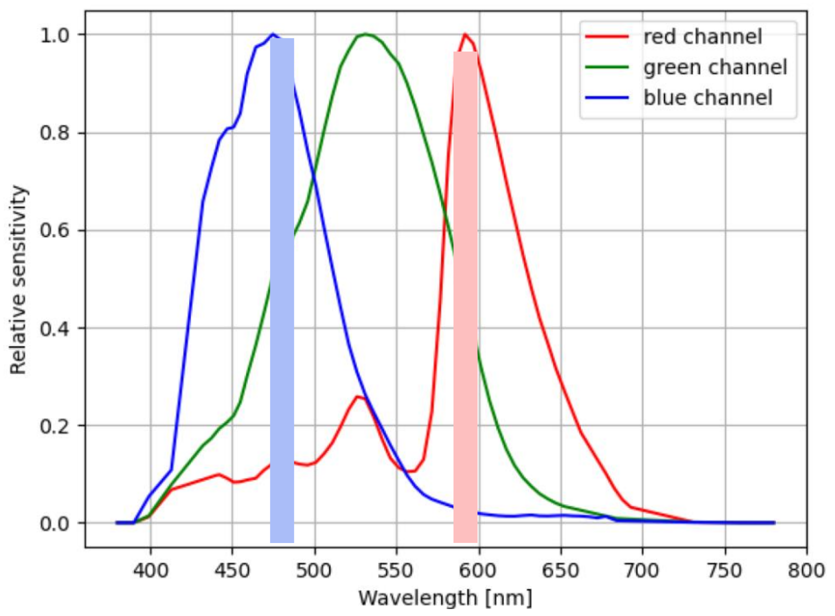



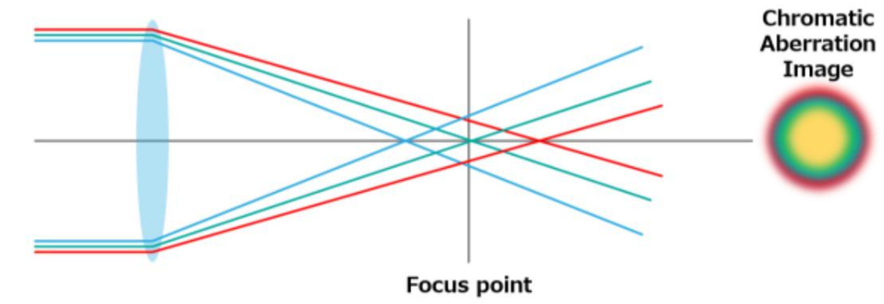


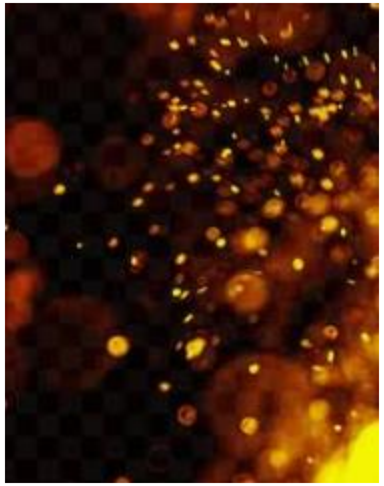

- Different camera channels are sensitive to different (overlapping) spectral ranges
- A dual or triple bandpass filter may be installed to improve camera pyrometry performance.
- Camera can be calibrated with a black-body or ribbon lamp (spatially uniform source).
- A camera sensor consists of a square pattern of R,G,B pixels, with gaps in between.
- Image of some particles in a dust flame are focused onto the sensor. If you change the focal distance, other particles become focused.
- R, G, B signals ratios do not correspond to particle temperatures (see illustration).
- Chromatic aberrations make it even worse.

# Color camera pyrometry. Cameras with 3 or more sensors.

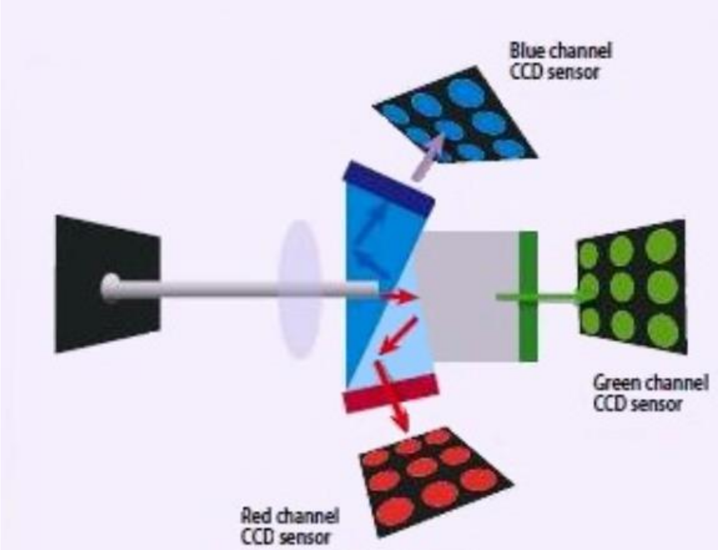


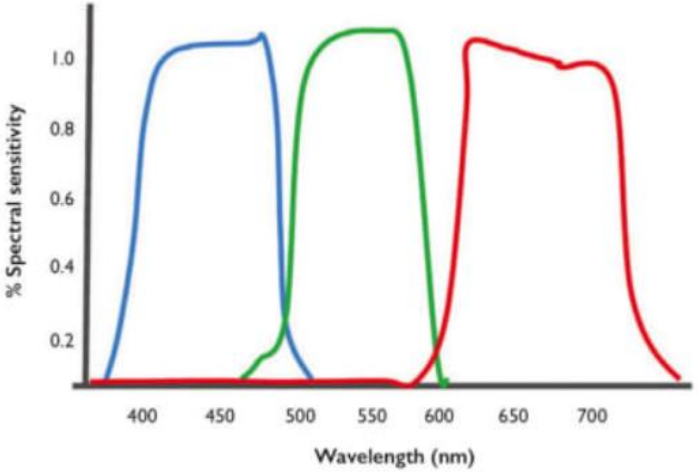


- Light is split on 3 or more channels and focused on separate B/W sensors, each one equipped with a bandpass filter.
- If separate sensors are perfectly aligned, then R, G, B… ratios will depend on the particle temperature only.
- Bur the alignment precision is ~ 0.5-pixel size, meaning that the problem remains.

# Color camera pyrometry. Possible solutions.

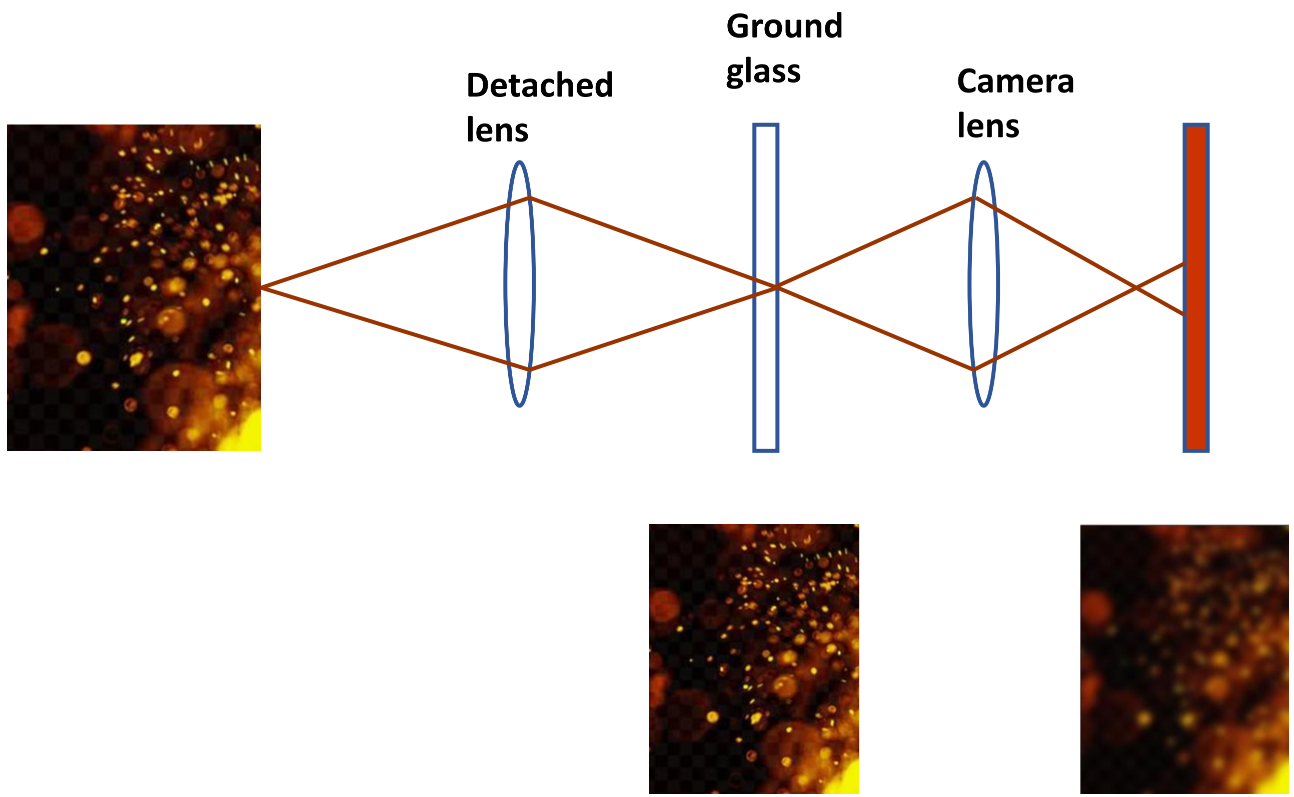


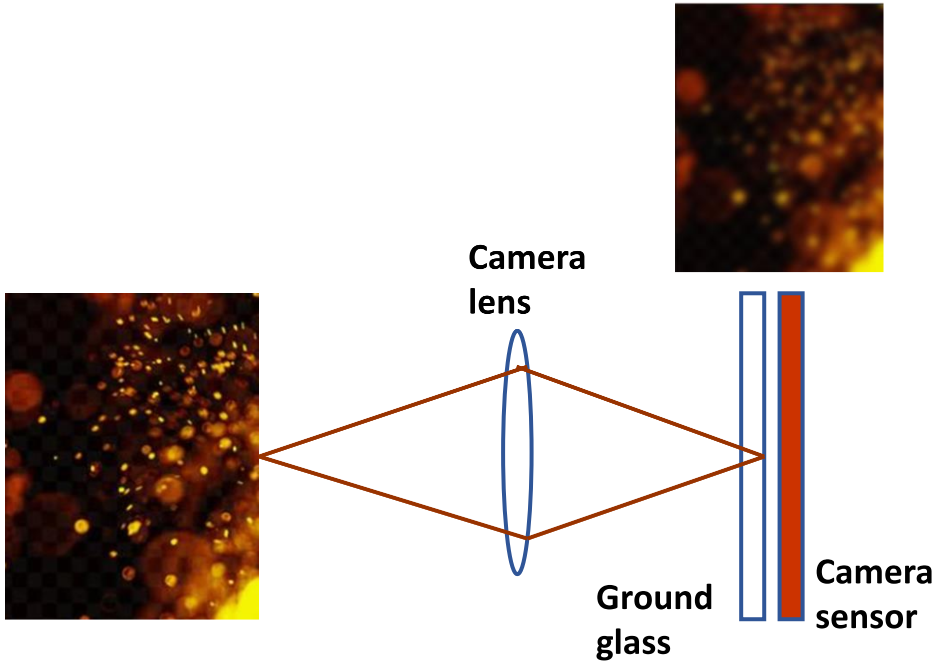


- May be tried, but no warranty that it works.